Article
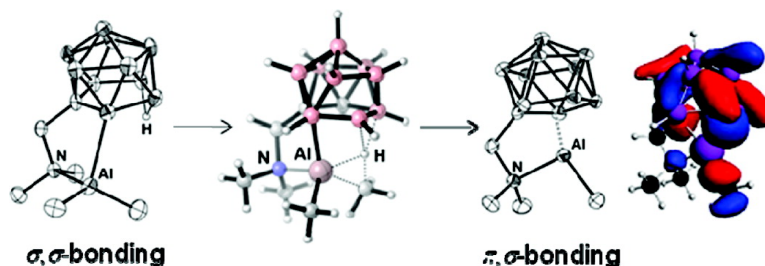
# Dicarbollylamine Ligand as a Tunable Template for #,#- and #,#-Bonding Modes: Syntheses, Structures, and Theoretical Studies of #:#-Coordinated Constrained-Geometry Group 13 Metal Complexes

Jong-Dae Lee, Sung-Kwan Kim, Tae-Jin Kim, Won-Sik Han, Young-Joo Lee, Dae-Hwan Yoo, Minserk Cheong, Jaejung Ko, and Sang Ook Kang

σ,σ-bonding        π,σ-bonding

## More About This Article

Additional resources and features associated with this article are available within the HTML version:

- Supporting Information
- Access to high resolution figures
- Links to articles and content related to this article
- Copyright permission to reproduce figures and/or text from this article

View the Full Text HTML

# Dicarbollylamine Ligand as a Tunable Template for σ,σ- and π,σ-Bonding Modes: Syntheses, Structures, and Theoretical Studies of $\eta^5$:$\eta^1$-Coordinated Constrained-Geometry Group 13 Metal Complexes

Jong-Dae Lee,[†] Sung-Kwan Kim,[‡] Tae-Jin Kim,[‡] Won-Sik Han,[‡] Young-Joo Lee,[‡]
Dae-Hwan Yoo,[‡] Minserk Cheong,[§] Jaejung Ko,*[,‡] and Sang Ook Kang*[,‡]

*Department of Chemistry, College of Natural Science, Chosun University, 375 Dong-gu,
Gwangju 501-759, South Korea, Department of Chemistry, Korea University, 208 Seochang,
Chochiwon, Chung-nam 339-700, South Korea, and Department of Chemistry and Research
Institute for Basic Sciences, Kyung Hee University, Seoul 130-701, South Korea*

Received March 29, 2008; E-mail: sangok@korea.ac.kr

***Abstract:*** A series of group 13 main group complexes with π,σ-type bonding interaction of the formula [{($\eta^5$-RC$_2$B$_9$H$_9$)(CH$_2$)($\eta^1$-NMe$_2$)}MMe] (M = Al, R = H **5**, Me **6**; Ga, R = H **7**, Me **8**; In, R = H **9**, Me **10**) was produced by the reaction of group 13 metal alkyls (MMe$_3$; M = Al, Ga, In) with the dicarbollylamine ligands, *nido*-8-R-7,8-C$_2$B$_9$H$_{10}$-7-(CH$_2$)NHMe$_2$ (R = H **1**, Me **2**). The reactions of **1** and **2** with AlMe$_3$ in toluene initially afforded tetra-coordinated aluminum complexes with σ,σ-type bonding interaction, [{($\eta^1$-RC$_2$B$_9$H$_{10}$)(CH$_2$)($\eta^1$-NMe$_2$)}AlMe$_2$] (R = H **3**, Me **4**), which readily underwent further methane elimination to yield the corresponding constrained geometry complexes (CGCs, **5** and **6**) of aluminum with π,σ-bonding interaction. However, the reactions between **1** and **2** and MMe$_3$ (M = Ga, In) in toluene produced gallium and indium π,σ-CGCs of **7** and **10** directly, not proceeding through σ,σ-intermediates. The structures of group 13 metal CGCs were established by X-ray diffraction studies of **5**, **6**, and **8**, which authenticated a characteristic $\eta^5$:$\eta^1$-coordination mode of the dicarbollylamino ligand to the group 13 metals. A similar π,σ-bonding interaction was also established in ethylene-bridged dicarbollylethylamine series. Thus, aluminum π,σ-CGCs of dicarbollylethylamine, [{($\eta^5$-RC$_2$B$_9$H$_9$)(CH$_2$)$_2$($\eta^1$-NBz$_2$)}AlMe] (R = H **17**, Me **18**), were prepared by the trans-metalation of the [{($\eta^5$-RC$_2$B$_9$H$_9$)(CH$_2$)$_2$($\eta^1$-NBz$_2$)}Ti(NMe$_2$)$_2$] (R = H **15**, Me **16**) with AlMe$_3$. However, only σ,σ-bonded complexes of the formula [{($\eta^1$-RC$_2$B$_9$H$_9$)(CH$_2$)$_2$($\eta^1$-NBz$_2$)}AlMe$_2$] (R = H **13**, Me **14**) were isolated by the reaction between [*nido*-7-8-R-7,8-C$_2$B$_9$H$_{10}$-(CH$_2$)$_2$HNBz$_2$] (R = H **11**, Me **12**) and AlMe$_3$. When methane-elimination reactions between metal alkyls and dicarbollylamines were carried out with either the gallium atom or monobenzyl aminoethyl tethered ligands, [*nido*-7-H$_2$NBz(CH$_2$)$_2$-8-R-7,8-C$_2$B$_9$H$_{10}$] (R = H **21**, Me **22**), desired π,σ-CGCs, [{($\eta^5$-RC$_2$B$_9$H$_9$)(CH$_2$)$_2$($\eta^1$-NBz$_2$)}GaMe] (R = H **19**, Me **20**) or [{($\eta^5$-RC$_2$B$_9$H$_9$)(CH$_2$)$_2$($\eta^1$-NHBz$_2$)}AlMe] (R = H **23**, Me **24**), were generated, respectively. DFT calculation on **5** provides evidence of existence of π,σ-bonding of dicarbollylamine ligand to the aluminum atom: π-bonding interaction of a dicarbollyl unit becomes intensified in the presence of a weak σ-bonding amine-tethered group. Furthermore, preference for the formation of π,σ-bonding was predicted by optimizing a reaction profile including σ,σ- and π,σ-structures as well as transition state structures for each methylene- and ethylene-spaced ligand system, **3**−**5** and **14**−**18**, to reveal that π,σ-bonding interaction is more favorable in the case of a methylene-tethered ligand system.

## Introduction

The great success of constrained-geometry catalysts in the polyolefin industry[1] has led to interest in developing main group metal analogues of these catalysts.[2] One of the reference catalysts is the titanium complex [($\eta^5$-Me$_4$C$_5$)Me$_2$Si($\eta^1$-BuN$^t$)]TiCl$_2$, which represents a characteristic π,σ-bonding interaction at the titanium metal center. The term "constrained geometry" is derived from the half-sandwich structure of these complexes, in which one ancillary ligand tethered to the cyclopentadienide ring functions as a σ-donor.[3a] The unique combination of π,σ-coordination is believed to facilitate the
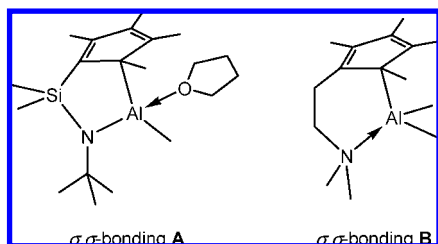
---

† Chosun University.
‡ Korea University.
§ Kyung Hee University.

(1) (a) McKnight, A. L.; Waymouth, R. M. *Chem. Rev.* **1998**, *98*, 2587. (b) Siemeling, U. *Chem. Rev.* **2000**, *100*, 1495. (c) Braunschweig, H.; Breitling, F. M. *Coord. Chem. Rev.* **2006**, *250*, 2691.

(2) (a) Jutzi, P.; Dahlhaus, J.; Bangel, M. *J. Organomet. Chem.* **1993**, *460*, C13. (b) Jutzi, P.; Dahlhaus, J.; Neumann, B.; Stammler, H. G. *Organometallics* **1996**, *15*, 747. (c) Pietryga, J. M.; Gorden, J. D.; Macdonald, C. L. B.; Voigt, A.; Wiacek, R. J.; Cowley, A. H. *J. Am. Chem. Soc.* **2001**, *123*, 7713. (d) Wiacek, R. J.; Macdonald, C. L. B.; Jones, J. N.; Pietryga, J. M.; Cowley, A. H. *Chem. Commun.* **2003**, 430. (e) Pietryga, J. M.; Jones, J. N.; Mullins, L. A.; Wiacek, R. J.; Cowley, A. H. *Chem. Commun.* **2003**, 2072.

**Chart 1.** Previous Examples of σ,σ-Bonded Aluminum Complexes, **A** and **B**



**Scheme 1.** Generation of π,σ-CGCs (**5** and **6**) via σ,σ-Bonded Complexes (**3** and **4**)



incorporation of various α-olefins into growing polymer chains.[3] Among the main group elements, group 13 metals are of special interest due to their general utilities as alternate catalytic systems for olefin polymerization.[4] Until now, however, no constrained geometry group 13 metal complexes with $\eta^5$:$\eta^1$-coordination had been structurally characterized. Previously, only $\eta^1$:$\eta^1$-coordinated aluminum complexes of the types **A** and **B** have been structurally characterized in cyclopentadienide systems containing either an amido[2c] or amine[2b] tethering unit, as shown in Chart 1.

Among group 13 elements, the aluminum atom appears to be particularly flexible in its coordination with a cyclopentadienyl ring, in that examples of cyclopentadienyl aluminum complexes $\eta^1$-,[5] $\eta^2$-,[6] $\eta^3$-,[7] and $\eta^5$-[8] geometries have all been characterized.[9] However, in the case of complexes **A** and **B**, the electronic influence of the amido or amine tether should directly inhibit the formation of a π-bonding between the cyclopentadienyl ring and aluminum atom, thereby only providing a σ,σ-bonding in the ground-state structure of the molecule.

In the search for new types of ligand systems for which π,σ-coordination may be plausible, the dicarbollyl moiety has been employed as a π-bonding group instead of the cyclopentadienyl ligand (Cp). The dicarbollide anion is a versatile ligand that is an isolobal inorganic analogue of the Cp$^-$ ion. Preparing constrained-geometry complexes with this dicarbollyl functionality is a challenging project since incorporation of a dicarbollyl fragment into the ligand framework will create new metal/charge combinations. The formal replacement of the monoanionic Cp$^-$ ligand in [CpM(III)]$^{+2}$ with the isolobal, dianionic dicarbollyl ligand $(C_2B_9H_{11})^{-2}$ to give a $[(C_2B_9H_{11})M(III)]^{+1}$ fragment reduces the overall charge by one unit but leaves the gross structural and metal frontier orbital properties unchanged.
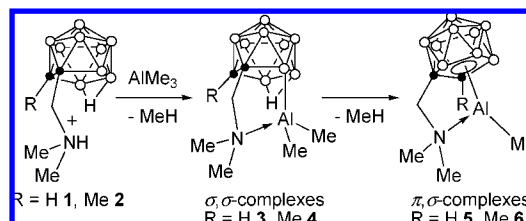
Consequently, complex design of this type can potentially be used to control secondary metal/ligand interactions; the weaker ionic character of the pendent neutral amino group enhances the metal's π-bonding capability with the dicarbollyl ligand through an $\eta^5$-coordination. Thus, it was predicted that incorporation of the dicarbollyl fragment into the ligand framework would enable construction of constrained-geometry group 13 metal complexes with unprecedented π,σ-bonding interaction.

Based on this assumption dicarbollylmethylamine ligand systems (**1** and **2**) were studied to show that the desired aluminum π,σ-CGCs (**5** and **6**) were achieved. In addition, during the reaction, σ,σ-bonded complexes (**3** and **4**) were also isolated, and their $\eta^1$:$\eta^1$-coordination was confirmed based on crystallographic studies. Further application of these ligand systems to gallium and indium atoms successfully led to the isolation of corresponding π,σ-bonded CGCs of gallium and indium. As an extension of ligand variation, ethylene-bridged dicarbollylethylamine systems were studied, and a reversed trend of stability between σ,σ- and π,σ-bonding was found upon the aluminum coordination. When dicarbollyl-N,N′-dibenzylethylamine ligands (**11** and **12**) were reacted with trimethyl aluminum (TMA), only σ,σ-bonded complexes (**13** and **14**) were isolated even under the prolonged reaction condition. To obtain the desired aluminum π,σ-CGCs, trans-metalation reactions were devised in the frame of $\eta^5$:$\eta^1$-coordinated titanium CGCs. However, when a less bulky N-monobenzylaminoethyl tethered group (**11** and **12**) was employed, desired aluminum π,σ-CGCs (**23** and **24**) were successfully isolated. On the contrary, the π,σ-bonding pattern of the gallium atom (**19** and **20**) is invariant regardless of size of the bridging unit (Figure 1).

## Results and Discussion

Ligand systems, dicarbollyl-N,N′-dimethyl-methylamines (**1** and **2**), consisted of two dissimilar coordination modes of dicarbollyl, and ammine functionalities were produced based on the standard deboronation procedure by reacting o-carboranyl-N,N′-dimethyl-methylamine with KOH in an ethanol solution. Treatment of **1** and **2**[10] with 1 equiv of TMA in toluene at reflux for 10 h gave aluminum π,σ-bonded CGCs of the general formula $[(\eta^5\text{-RC}_2B_9H_9)CH_2(\eta^1\text{-NMe}_2)]Al(Me)$ (R = H **5**, Me **6**) in good yield (Scheme 1).

While monitoring the reaction progress by $^1$H NMR, we observed the exclusive formation of σ,σ-bonded complexes in an early stage and subsequent transformation to π,σ-bonded complexes. Thus, a facile formation of σ,σ-complexes was confirmed by a short reaction condition, only requiring an hour to form **3** and **4** from the reaction between **1** and **2** and TMA. As shown in Table 1, $^1$H NMR spectra of **3** and **4** contain two

(3) (a) Sapiro, P. J.; Bunel, E.; Schaefer, W. P.; Bercaw, J. E. *Organometallics* **1990**, *9*, 867. (b) Okuda, J. *Chem. Ber.* **1990**, *123*, 1649. (c) Hughes, A. K.; Meetsma, A.; Teuben, J. H. *Organometallics* **1993**, *12*, 1936. (d) Chen, Y. X.; Stern, C. L.; Yang, S.; Marks, T. J. *J. Am. Chem. Soc.* **1996**, *118*, 12451. (e) Alt, H. G.; Reb, A.; Milins, W.; Weis, A. *J. Organomet. Chem.* **2001**, *628*, 169.

(4) (a) Lanza, G.; Fragalà, I. L.; Marks, T. J. *J. Am. Chem. Soc.* **1998**, *120*, 8257. (b) Dagorne, S.; Guzei, I. A.; Coles, M. P.; Jordan, R. F. *J. Am. Chem. Soc.* **2000**, *122*, 274. (c) Korolev, A. V.; Ihara, E.; Guzei, I. A.; Young, V. G., Jr.; Jordan, R. F. *J. Am. Chem. Soc.* **2001**, *123*, 8291.

(5) Dohmeier, C.; Schnöckel, H.; Robl, C.; Schneider, U.; Ahlrichs, R. *Angew. Chem.* **1993**, *105*, 1714.

(6) Drew, D. A.; Haaland, A. *Chem. Commun.* **1972**, 1300.

(7) Fisher, J. D.; Shapiro, P. J.; Budzelaar, P. H. M.; Staples, R. *J. Inorg. Chem.* **1998**, *37*, 1295.

(8) (a) Teclé, B.; Corfield, P. W. R.; Oliver, J. P. *Inorg. Chem.* **1982**, *21*, 458. (b) Schulz, S.; Häming, L.; Herbst-Irmer, R.; Roesky, H. W.; Sheldrick, G. M. *Angew. Chem.* **1994**, *106*, 1052. (c) Fisher, J. D.; Shapiro, P. J.; Yap, G. P. A.; Rheingold, A. L. *Inorg. Chem.* **1996**, *35*, 271.

(9) See also: Budzelaar, P. H. M.; Engelberts, J. J.; Lenthe, J. H. v. *Organometallics* **2003**, *22*, 1562.

(10) (a) Kim, D.-H.; Won, J. H.; Kim, S.-J.; Ko, J.; Kim, S. -H.; Cho, S.; Kang, S. O *Organometallics* **2001**, *20*, 4298. (b) Lee, J.-D.; Lee, Y.-J.; Son, K. C.; Cheong, M.; Ko, J.; Kang, S. O. *Organometallics* **2007**, *26*, 3374.

**Table 1.** Comparison of the NMR Spectroscopic Data for Compounds **1**−**10**

| compd | $^1$H NMR ($\delta$) | | | | $^{13}$C NMR ($\delta$) | | |
|---|---|---|---|---|---|---|---|
| | CH$_2$ | NMe$_2$ | M−Me | B−H−B | CH$_2$ | NMe$_2$ | M−Me |
| **1**$^a$ | 2.92, 3.31 | 2.70 | | −3.01 | 54.92 | 43.55, 44.63 | |
| **2**$^a$ | 2.72, 2.80 | 2.50 | | −2.82 | 57.57 | 42.96, 47.82 | |
| **3**$^c$ | 2.27, 2.59 | 1.49, 1.74 | −0.17, −0.53 | −3.20 | 67.94 | 45.75, 46.45 | −8.60, −9.93 |
| **4**$^c$ | 2.46, 2.68 | 1.66, 1.84 | −0.20, −0.39 | −3.03 | 62.94 | 46.51, 46.70 | −7.82, −10.07 |
| **5**$^b$ | 1.72, 2.05 | 1.34, 1.64 | −0.19 | | 63.72 | 42.97, 46.61 | −7.42 |
| **6**$^b$ | 1.97, 2.17 | 1.48,1.84 | −0.21 | | 53.75 | 45.75, 47.60 | −6.92 |
| **7**$^c$ | 1.85, 2.23 | 1.64, 1.87 | 0.42 | | 64.91 | 46.32, 46.37 | 1.32 |
| **8**$^c$ | 1.89, 2.24 | 1.75, 2.02 | 0.38 | | 60.25 | 46.06, 47.63 | 1.38 |
| **9**$^c$ | 2.00, 2.17 | 1.42, 1.70 | 0.11 | | 65.91 | 46.04, 46.53 | 1.32 |
| **10**$^c$ | 1.90, 2.18 | 1.82, 1.94 | 0.45 | | 64.90 | 47.25, 47.31 | 1.61 |

$^a$ (CD$_3$)$_2$SO was used as the solvent, and the chemical shifts are reported relative to the residual H of the solvent. $^b$ C$_6$D$_6$ was used as the solvent, and the chemical shifts are reported relative to the residual H of the solvent. $^c$ CD$_3$C$_6$D$_5$ was used as the solvent, and the chemical shifts are reported relative to the residual H of the solvent.
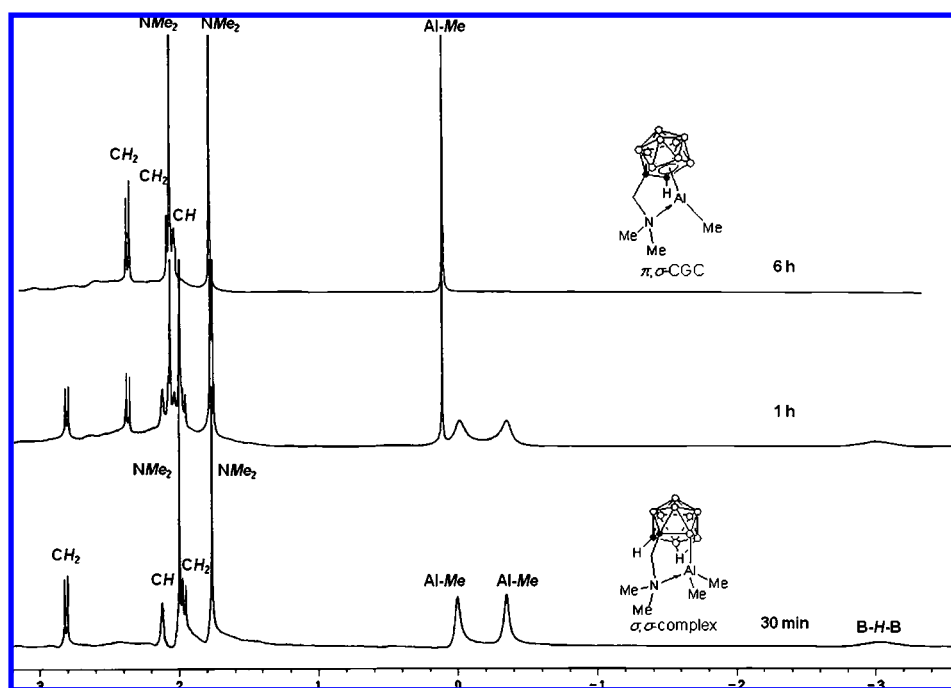


**Figure 1.** Characteristic NMR chemical shift changes from conversion of $\sigma,\sigma$- to $\pi,\sigma$-aluminum dicarbollide complexes.

distinctive Al−Me peaks at around $\delta$ −0.17 to −0.53 and a bridging hydrogen peak at around $\delta$ −3.03 to −3.20, indicating only one methyl group on TMA was removed. Disappearance of a NH proton and an upfield shift of methyl groups of NMe$_2$ indicate the presence of dative $\sigma$-bonding of Me$_2$N → Al. Thus, asymmetric $\sigma,\sigma$-bonded structures were proposed based on the observation of the diastereotopic splitting pattern of the methylene unit and two separate methyl resonances for the coordinated amino functionality (CH$_2$NMe$_2$). Prolonged reaction proceeded to the formation of stable $\pi,\sigma$-complexes. X-ray structural studies authenticated $\eta^1$:$\eta^1$- and $\eta^5$:$\eta^1$-type interactions at the aluminum center (see Figure 2 for **3** and Figures 3 and 4 for CGCs **5** and **6**).

Figure 1 portrays a sequential conversion process for **3** from $\sigma,\sigma$- to stable $\pi,\sigma$-complexes. Within 1 h of refluxing, the disappearance of B−H−B and two Al−Me resonance signals of **3** was noticeable in the $^1$H NMR spectra. One of the notable features for the transformation of **3** to **5** was the spectral change arisen from diastereotopic methylene resonances: The values of each coupling constant for $^1J_{C−H}$ and $^2J_{H−H}$ decreases from 255 and 7 Hz to 88 and 6 Hz, respectively. In addition, widely scattered signals related to dicarbollylmethylamine in **3** was

curtailed in a smaller range, alluding the formation of $\pi$-coordination of the aluminum atom in **5**. Transformation to **5** was completed within 6 h of refluxing with toluene.

A similar protocol was applied to the preparation of gallium $\pi,\sigma$-bonded CGCs as shown is Scheme 2. Addition of trimethylgallium (TMG) to the toluene solution of **1** and **2** resulted in the formation of $\sigma,\sigma$-bonded intermediates as seen in aluminum reactions. In the case of gallium, even though the formation of a $\sigma,\sigma$-bonded intermediate was discernible in $^1$H NMR spectra, reaction always proceeded to completion forming $\pi,\sigma$-bonded CGCs in shorter reaction times. Isolation of $\sigma,\sigma$-bonded intermediates was attempted, but gallium preferred to form $\pi,\sigma$-CGC structures instead. $^1$H NMR spectra comprise all common traits of the formation of gallium $\pi,\sigma$-CGCs, exhibiting a characteristic shift and splitting patterns of CH$_2$N and NMe$_2$ units as found in entries of **7** and **8** in Table 1. Final unequivocal evidence of a $\pi,\sigma$-bonding interaction was provided by an X-ray structural study of **7**, revealing an $\eta^5$:$\eta^1$-coordination geometry (Figure 5).
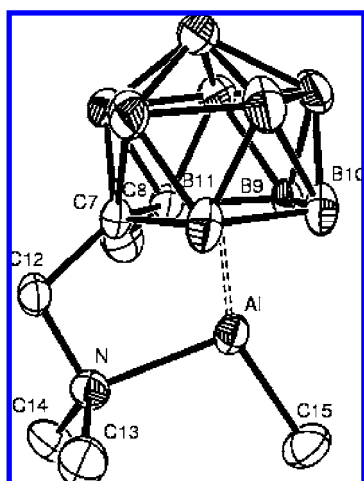
Indium $\pi,\sigma$-bonded CGCs were also produced from the same synthetic protocol (Scheme 2). Similar to the reaction of gallium, $\sigma,\sigma$-intermediate and $\pi,\sigma$-bonded CGCs were identified even
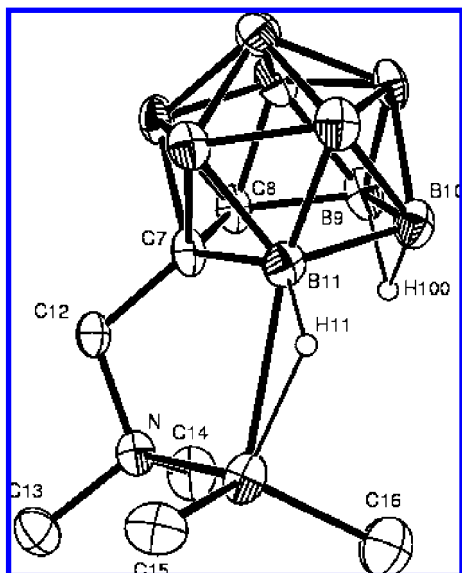
**Figure 2.** Molecular structure of **3** with thermal ellipsoids drawn at the 30% level.
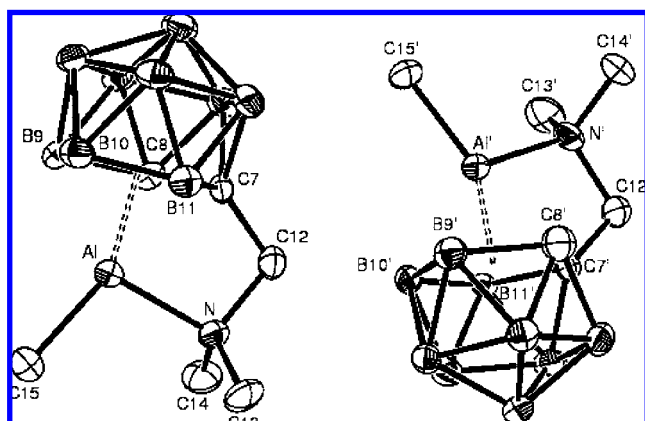


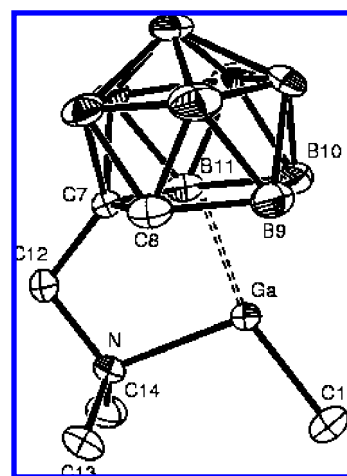**Figure 3.** Molecular structure of **5** with thermal ellipsoids drawn at the 30% level.



**Figure 4.** Molecular structure of **6** with thermal ellipsoids drawn at the 30% level.

in a shorter reaction time, based on $^1$H NMR characterization. As shown in Table 1, indium π,σ-bonded CGCs (**9** and **10**) exhibit characteristic shifts and splitting patterns of In–*Me*, CH$_2$N, and N*Me*$_2$ groups.

**Scheme 2.** Selective Formation of Gallium and Indium π,σ-CGCs
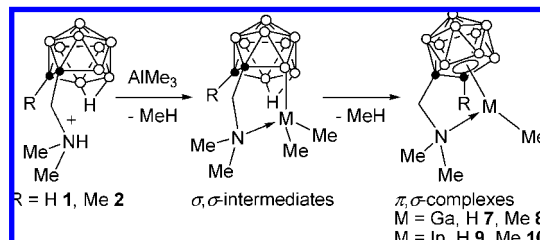


Based on the assumption that special features on a constrained geometry come from the bridging unit between two dissimilar coordination units capable of accommodating π,σ-bonding interaction, variation on the bridging unit from methylene to ethylene may perturb the stability balance between σ,σ- and π,σ-bonding interactions. Since group 13 atoms are known to bound a Cp anionic ligand in such a manner, a new template with dicarbollyl and amine functional groups modulated by elongation of spacer in between is of special interest. In accordance to our expectation, only σ,σ-bonded complexes were produced from the reaction of aluminum with ethylene-bridged ligands, dicarbollyethylamines (**11** and **12**). Thus, even under prolonged refluxing reactions of **11** and **12** with TMA, desired π,σ-CGCs of aluminum were not formed, only resulting in σ,σ-bonded complexes (**13** and **14**) (Scheme 3). σ,σ-Bonded complexes (**13** and **14**) were proposed based on the assignment of $^1$H NMR resonances (Table 2). A σ-bonding interaction between the aluminum atom and dicarbollide functionality comes from the observation of resonance signals at around δ −3.0 and −0.1 to −0.5 for B–H–B and two units of Al–*Me*$_2$, respectively. Another σ-type dative-bonding interaction is originated from an amine tether and evidenced by an upfield



**Figure 5.** Molecular structure of **7** with thermal ellipsoids drawn at the 30% level.

**Scheme 3.** New Templates Containing Ethylene-Bridging Unit for Stablilizing σ,σ-Bonded Complexes (**13** and **14**)
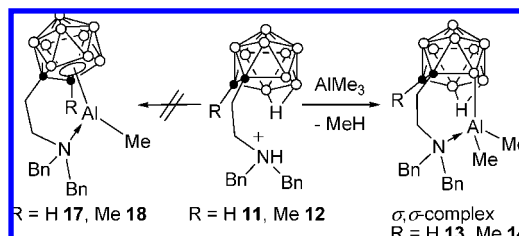
**Table 2.** Comparison of the NMR Spectroscopic Data for Compounds **11**−**24**

| compd | CH$_2$CH$_2$ | $^1$H NMR ($\delta$) CH$_2$Ph | CH$_2$*Ph* | M−*Me* | B−*H*−B | CH$_2$CH$_2$ | $^{13}$C NMR ($\delta$) CH$_2$Ph | Ph | M−*Me* |
|---|---|---|---|---|---|---|---|---|---|
| **11**$^a$ | 1.90, 2.96 | 4.30 | 7.36−7.48 |  | −3.12 | 31.53, 45.01 | 56.14 | 128.99−131.12 |  |
| **12**$^a$ | 1.96, 3.01 | 4.35 | 7.36−7.49 |  | −2.91 | 28.36, 50.64 | 56.54 | 129.14−131.32 |  |
| **13**$^b$ | 1.88, 2.17, 3.73, 4.23 | 3.51,3.80 | 7.24−7.36 | −0.12,−0.47 | −3.31 | 37.51, 51.24 | 61.32,62.86 | 125.15−138.37 | −5.63,−3.87 |
| **14**$^b$ | 1.90, 2.22, 3.67, 4.18 | 3.54,3.82 | 7.27−7.35 | −0.24,−0.45 | −3.08 | 38.46, 51.90 | 62.02,64.57 | 125.52−139.34 | −5.53,−4.77 |
| **17**$^b$ | 1.98, 2.14, 3.58, 4.20 | 3.40,3.80 | 7.34−7.45 | −−0.23 |  | 32.88, 49.72 | 61.82,64.44 | 125.27−139.46 | −3.28 |
| **18**$^b$ | 2.04, 2.27, 3.65, 4.27 | 3.47,3.77 | 7.36−7.48 | −0.30 |  | 37.47, 48.83 | 61.49,63.91 | 125.21−138.96 | −2.36 |
| **19**$^b$ | 2.08, 2.17, 3.59, 4.18 | 3.41,3.69 | 7.35−7.43 | 0.39 |  | 34.69, 47.92 | 62.17,65.53 | 125.19−139.22 | 0.58 |
| **20**$^b$ | 2.01, 2.23, 3.68, 4.24 | 3.44,3.78 | 7.36−7.46 | 0.32 |  | 34.77, 48.09 | 61.22,65.37 | 125.31−139.79 | 0.74 |
| **21**$^a$ | 1.87, 2.88 | 4.20 | 7.30−7.40 |  | −2.99 | 31.21, 51.35 | 58.82 | 129.18−132.57 |  |
| **22**$^a$ | 1.92, 2.97 | 4.17 | 7.35−7.47 |  | −2.89 | 30.74, 50.02 | 57.73 | 128.67−132.13 |  |
| **23**$^b$ | 2.07, 2.44, 3.57, 4.19 | 3.38,3.66 | 7.14−7.31 | −0.34 |  | 38.05, 49.71 | 62.35 | 125.94−140.35 | −1.24 |
| **24**$^b$ | 1.99, 2.20, 3.55, 4.12 | 3.42,3.72 | 7.21−7.39 | −0.37 |  | 38.55, 51.06 | 62.27 | 126.22−140.28 | −2.48 |

$^a$ (CD$_3$)$_2$SO was used as the solvent, and the chemical shifts are reported relative to the residual H of the solvent. $^b$ CD$_3$C$_6$D$_5$ was used as the solvent, and the chemical shifts are reported relative to the residual H of the solvent.
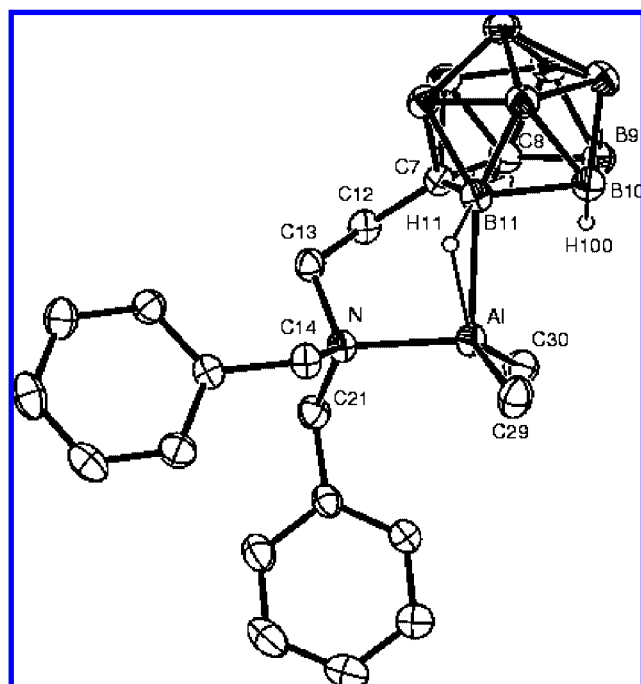


**Figure 6.** Molecular structure of **14** with thermal ellipsoids drawn at the 30% level.

shift of resonances associated with the methylene units attached to the nitrogen atom, revealing chemical shifts at around $\delta$ 1.8−4.2 and 3.5−3.8 for the ethylene-bridge and benzyl units on the amine, respectively. Furthermore, $\sigma$-dative bonding of an amine tether to the aluminum atom creates an asymmetric environment in the ligand backbone, featuring a diastereotopic splitting pattern of methylene units on both the ethylene spacer and benzyl substituents. An X-ray structural study on **14** confirmed the $\eta^1$:$\eta^1$-coordination between the aluminum and dicarbollylethylamine ligand (Figure 6), exhibiting a $\sigma$,$\sigma$-bonding interaction.

Much effort has been directed to the production of $\pi$,$\sigma$-CGCs, including applying prolonged reaction conditions. It has been realized that a trans-metalation between titanium and aluminum is facile in dicarbollyl ligand systems, taking advantage of the high negative charge of the dicarbollide anion. Indeed, trans-metalation proceeded smoothly by reacting titanium CGCs (**15** and **16**) with TMA to generate corresponding aluminum $\pi$,$\sigma$-bonded CGCs (**17** and **18**) where now two-carbon templates act as ancillary ligand systems (Scheme 4). Titanium $\pi$,$\sigma$-bonded

**Scheme 4.** Trans-metallation of Titanium CGCs with TMA to Give Corresponding $\pi$,$\sigma$-Bonded Aluminum CGCs **17** and **18**
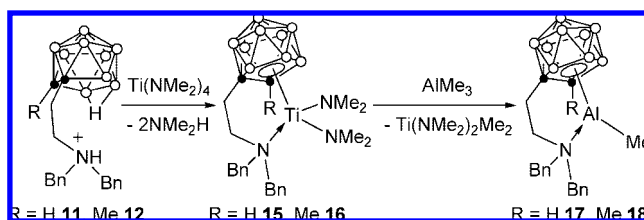


CGCs of this ligand were reported recently[11] and revealed that a flexible ethylene linker between dicarbollyl and amine functionalities posed an appropriate coordination angle for both $\eta^5$-dicarbollyl and $\eta^1$-amino units for titanium. Transformation to $\pi$,$\sigma$-bonded CGC structures was confirmed based on the assignment of chemical shifts from NMR study, revealing upfield resonances for ethylene units of the linker and methylene unit of aminobenzyl (entries **17** and **18** in Table 1). The final $\pi$,$\sigma$-bonding interaction was confirmed by an X-ray structural study of **18**, featuring an $\eta^5$:$\eta^1$-coordination at the aluminum center (Figure 7).

However, when TMG was tried, desired gallium $\pi$,$\sigma$-CGCs were exclusively produced as shown in Scheme 5. Similar $^1$H NMR spectral patterns for ethylene bridging unit and methylene of the benzyl group were observed in **19** and **20**. In addition, X-ray structural study confirmed the $\eta^5$:$\eta^1$-CGC structural features of **19** (Figure 8).

To reduce steric bulkiness arisen from dibenzyl functional group, monobenzyl substituted ligand systems, **11** and **12**, were studied. When reactions were carried out with TMA as well as **11** and **12**, desired aluminum $\pi$,$\sigma$-bonded CGCs (**23** and **24**) were exclusively produced (Scheme 6). X-ray structural study of **23** authenticated the $\eta^5$:$\eta^1$-coordination geometry as shown in Figure 9. Again, a spectral pattern as well as chemical shifts featuring $\pi$,$\sigma$-bonding interaction was discernible based on the $^1$H NMR analysis for the ethylene bridge, monobenzyl substituent, and amine hydrogen.

We have noticed that preference of $\pi$,$\sigma$-CGCs over $\sigma$,$\sigma$-CGCs depends on the central metals as well as the size of tethering groups and the bulkiness of the amine substituents as shown in Schemes 1–6. It is evident from the discussion thus far that templates with a methylene bridge and methyl substituent are very effective for stabilizing group 13 elements with $\pi$,$\sigma$-bonding.

(11) Lee, Y.-J.; Lee, J.-D.; Jeong, H.-J.; Son, K.-C.; Ko, J.; Cheong, M.; Kang, S. O. *Organometallics* **2005**, *24*, 3008.
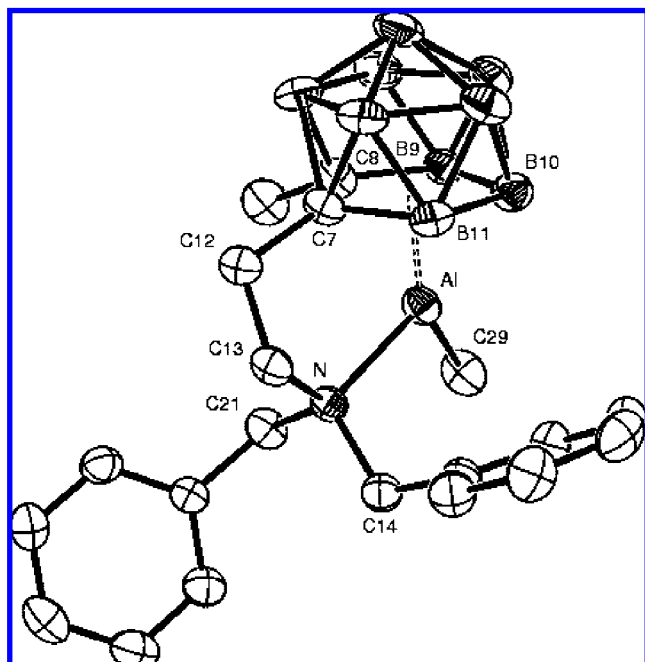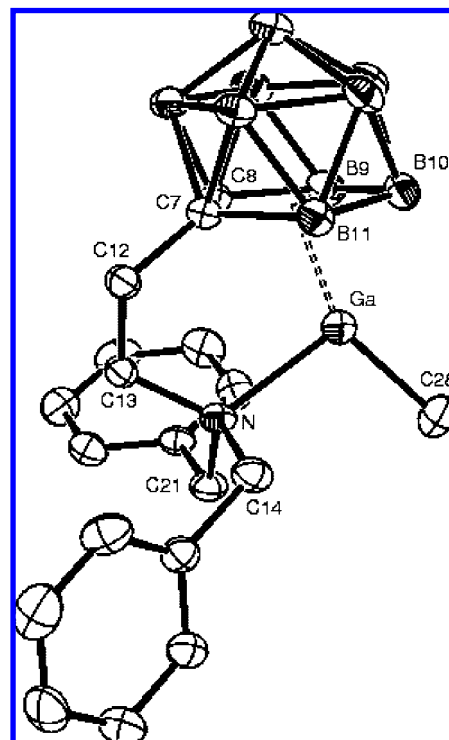
**Figure 7.** Molecular structure of **18** with thermal ellipsoids drawn at the 30% level.

**Scheme 5.** Generation of π,σ-Bonded Gallium CGCs from Ethylene-Bridged Templates
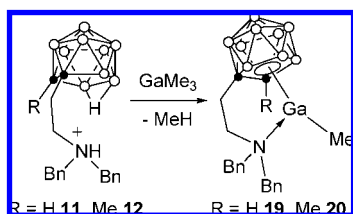


**X-ray Structural Studies on σ,σ- and π,σ-CGCs.** X-ray structural studies confirmed the geometries characteristic for $\eta^1$:$\eta^1$-type complexes and $\eta^5$:$\eta^1$-type CGCs. These included $\eta^1$:$\eta^1$-type (**3** and **14**) and $\eta^5$:$\eta^1$-type CGCs complexes (**5**, **6**, **7**, **18**, **19**, and **23**). Some general structural features are compared in Tables 3–6, where selected bond distances and angles on each ligand system, methylene and ethylene tethers, are separately presented in Tables 5 and 6, respectively. Detailed information on structural determinations and the structural features of all eight compounds discussed here is provided in the Supporting Information.

An X-ray analysis of **3** indicates σ,σ-bonding interactions, where there is an attachment of the aluminum atom to the boron atom on the dicarbollyl ring and the nitrogen atom of tethered methylamine. Such a σ,σ-bonding permits the formation of a five-membered Al−B−C−C−N ring (Figure 2). Moreover, one B−H terminal hydrogen is located between the aluminum and the B11 atoms hence indicating agostic interaction[12] with the electron-deficient aluminum center. The geometry at aluminum is a distorted tetrahedral with constrained angles of 85.3(2)°,

(12) (a) Young, D. A. T.; Wiersema, R. J.; Hawthorne, M. F. *J. Am. Chem. Soc.* **1971**, *93*, 5687. (b) Schubert, D. M.; Bandman, M. A.; Rees, W. S., Jr.; Knobler, C. B.; Lu, P.; Nam, W.; Hawthorne, M. F. *Organometallics* **1990**, *9*, 2046. (c) Demachy, I.; Volatron, F. *Eur. J. Inorg. Chem.* **1998**, 1015. (d) Cowley, A. R.; Downs, A. J.; Marchant, S.; Macrae, V. A.; Taylor, R. A. *Organometallics* **2005**, *24*, 5702.



**Figure 8.** Molecular structure of **19** with thermal ellipsoids drawn at the 30% level.

**Scheme 6.** Generation of Aluminum π,σ-Bonded CGCs from Mono-benzylamine Tether
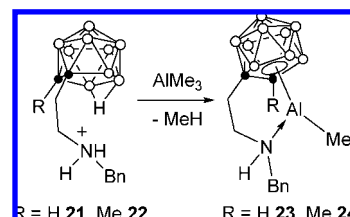


and the nitrogen geometry is a regular tetrahedral within a small range of variation [108.3(4)°−110.7(3)°]. Also, the endocyclic C7−C12−N bond angle is 110.9(4)°, which is within a small range of variation from the tetrahedral $sp^3$-C value. The structure of **3** resembles the complex [($\eta^1$-Cp*)(CH$_2$)$_2$($\eta^1$-NMe$_2$)]Al(Me)$_2$ **B**[2b] in the sense that it has the σ,σ-bonding mode. This species is believed to be a kinetically stabilized complex intermediate in which there is initial σ-electronic interaction of the aluminum atom with the amine sidearm and the concomitant $\eta^1$-type bonding with neighboring dicarbollyl unit.

A comparison of general structural features of π,σ-CGCs with those of the methylene-spaced ligand system is given in Table 5. Complex **5** may serve as an example for outlining the general characteristics of this class of compounds. As shown in Figure 3, the asymmetric unit contains two molecules related by local twofold symmetry, and the structures of the two independent molecules are essentially identical. The central aluminum atom in **5** is coordinated to a methyl ligand and an amine nitrogen in a σ-bonding manner, while a dicarbollyl unit coordinates toward a π-bonding interaction. The Al−C(Me) and Al−N bonds are in a normal range, having values of 1.944 and 2.037 Å (av), respectively.[13] The aluminum metal is centered approximately
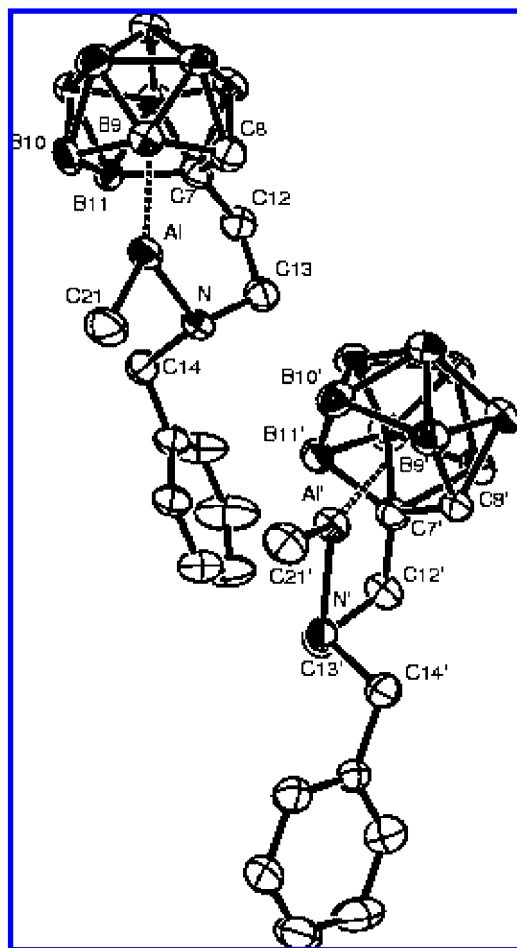
**Figure 9.** Molecular structure of **23** with thermal ellipsoids drawn at the 30% level.

over the ring, giving rise to an Al−C$_2$B$_3$ face (centroid) [where C$_2$B$_3$(centroid) is the centroid of the dicarbollyl ring] distance of 1.713 Å (av). The dicarbolly unit is symmetrically $\eta^5$-coordinated to the aluminum atom. Thus, the Al−C7 linkage [2.302 Å (av)] is similar to the Al−C8 bonds [2.253 Å (av)], which in turn are themselves similar to the Al−B9/B10/B11 bonding (for values, see Table 2) [in the range 2.216−2.200 Å (av)]. The connecting C7−C12 vector between the dicarbollyl ring and the C7 bridge is bent out of the dicarbollyl ligand plane toward the metal center. The corresponding C$_2$B$_3$(centroid)−C7−C12 angle amounts to 137.71°/137.96°. The endocyclic C7−C12−N bond angle is 103.6° (av), which is far away from the tetrahedral $sp^3$-C value. The "constrained geometry" character in a series of related compounds is probably best characterized by the C$_2$B$_3$(centroid)−metal−nitrogen angle ($\alpha$-angle in Table 5), which responds sensitively to steric and electronic changes at the metal center: in **5**, it amounts to 103.43°(av). The coordination geometry of the ligand nitrogen atom is distorted tetrahedral within the range 100.4°−112.7°.

(13) (a) Bradley, D. C.; Coumbarides, G.; Harding, I. S.; Hawkes, G. E.; Maia, I. A.; Motevalli, M. *J. Chem. Soc., Dalton Trans.* **1999**, 3553. (b) Doyle, D.; Gun'ko, Y. K.; Hitchcock, P. B.; Lappert, M. F. *J. Chem. Soc., Dalton Trans.* **2000**, 4093. (c) Fooken, U.; Khan, M. A.; Wehmschulte, R. J. *Inorg. Chem.* **2001**, *40*, 1316. (d) Su, W.; Kim, Y.; Ellern, A.; Guzei, I. A.; Verkade, J. G. *J. Am. Chem. Soc.* **2006**, *128*, 13727. (e) Andrews, P. C.; Calleja, S.; Maguire, M. *Polyhedron* **2006**, *25*, 1625. (f) Su, W.; Kobayashi, J.; Ellern, A.; Kawashima, T.; Verkade, J. G. *Inorg. Chem.* **2007**, *46*, 7953.

*Table 3.* X-ray Crystallographic Data and Processing Parameters for Compounds **3, 5, 6, 7, 14, 18, 19,** and **23**

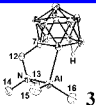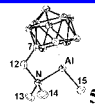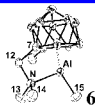| compd | 3 | 5 | 6 | 7 | 14 | 18 | 19 | 23 |
|---|---|---|---|---|---|---|---|---|
| formula | C$_7$H$_{24}$AlB$_9$N | C$_6$H$_{21}$AlB$_9$N | C$_7$H$_{23}$AlB$_9$N | C$_{13}$H$_{28}$B$_9$GaN | C$_{21}$H$_{37}$AlB$_9$N | C$_{20}$H$_{33}$AlB$_9$N | C$_{19}$H$_{31}$B$_9$GaN | C$_{30}$H$_{56}$Al$_2$B$_{18}$N$_2$ |
| formula weight | 246.54 | 231.51 | 245.53 | 365.37 | 427.79 | 411.74 | 440.46 | 693.31 |
| crystal system | orthorhombic | monoclinic | monoclinic | monoclinic | triclinic | triclinic | monoclinic | monoclinic |
| Z, space group | 4, $Pna2_1$ | 4, $P2_1$ | 4, $P2_1/n$ | 4, $P2_1/n$ | 2, $P\bar{1}$ | 2, $P\bar{1}$ | 4, $P2_1/n$ | 4, $P2_1/c$ |
| a/ Å | 19.109(7) | 7.205(1) | 7.887(9) | 9.578(1) | 8.525(4) | 8.524(1) | 11.815(8) | 18.770(4) |
| b/ Å | 7.275(3) | 16.460(2) | 15.625(2) | 11.701(1) | 10.739(5) | 9.517(1) | 13.824(1) | 12.377(3) |
| c/ Å | 11.101(4) | 11.882(2) | 12.352(2) | 17.972(2) | 14.128(6) | 14.591(2) | 13.916(1) | 18.571(4) |
| V, Å$^3$ | 1543.2(1) | 1399.6(3) | 1521.3(3) | 1990.1(4) | 1256.8(1) | 1149(3) | 2239.7(3) | 4074.3(2) |
| $\mu$/mm$^{-1}$ | 0.105 | 0.112 | 0.106 | 1.376 | 0.091 | 0.097 | 1.235 | 0.098 |
| crystal size/mm$^3$ | 0.25 × 0.14 × 0.12 | 0.25 × 0.15 × 0.12 | 0.31 × 0.25 × 0.14 | 0.35 × 0.25 × 0.14 | 0.29 × 0.21 × 0.11 | 0.21 × 0.20 × 0.15 | 0.22 × 0.21 × 0.14 | 0.46 × 0.30 × 0.26 |
| refl. collected/unique | 9254/3624 | 10 190/5299 | 10 914/3793 | 14 155/4934 | 9101/6106 | 7949/5611 | 16 164/5567 | 21 392/9357 |
| R(int) | 0.0955 | 0.0486 | 0.0477 | 0.0334 | 0.0262 | 0.1475 | 0.0513 | 0.1155 |
| R[$I > 2\sigma(I)$], wR2 | 0.0820, 0.1926 | 0.0579, 0.1392 | 0.0662, 0.1758 | 0.0972, 0.2399 | 0.0587, 0.1495 | 0.0780, 0.1542 | 0.0501, 0.1185 | 0.1034, 0.2426 |
| R (all data), wR2 | 0.1599, 0.2292 | 0.1200, 0.1658 | 0.1351, 0.2109 | 0.1409, 0.2803 | 0.1416, 0.1899 | 0.2808, 0.2158 | 0.1091, 0.1407 | 0.2688, 0.3404 |

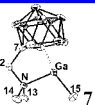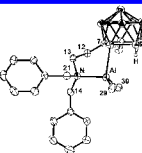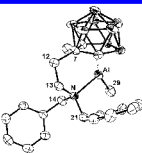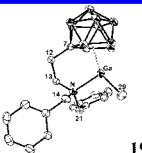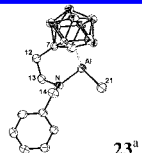**Table 4.** Compilation of Characteristic Structural Parameters of the **3**, **5**, **6**, **7**, **14**, **18**, **19**, and **23**[a]

| | 3 | 5 | 6 | 7 | 14 | 18 | 19 | 23 |
|---|---|---|---|---|---|---|---|---|
| M−C7 | | 2.303(4), 2.301(4) | 2.256(3) | | | 2.289(5) | | 2.458(5), 2.437(6) |
| M−C8 | | 2.270(4), 2.236(5) | 2.261(3) | 2.515(6) | | 2.273(5) | | 2.271(6), 2.335(6) |
| M−B9 | | 2.236(5), 2.196(5) | 2.240(3) | 2.236(8) | | 2.229(6) | 2.248(4) | 2.135(7), 2.174(7) |
| M−B10 | | 2.202(5), 2.198(5) | 2.207(4) | 2.123(7) | | 2.148(6) | 2.123(4) | 2.200(8), 2.156(7) |
| M−B11 | 2.481(6) | 2.199(5), 2.238(4) | 2.206(3) | 2.313(6) | 2.302(3) | 2.185(6) | 2.315(4) | 2.384(6), 2.254(7) |
| M−Cent | | 1.707, 1.718 | 1.703 | 1.833 | | 1.705 | 1.836 | 1.760, 1.788 |
| M−C(Me) | 1.909(5), 1.938(6) | 1.942(5), 1.946(5) | 1.927(3) | 1.949(8) | 1.960(3), 1.964(3) | 1.935(5) | 1.961(4) | 1.920(6), 1.931(6) |
| M−N | 1.996(4) | 2.037(4), 2.037(4) | 2.063(2) | 2.100(5) | 2.065(2) | 2.075(4) | 2.138(3) | 1.989(5), 1.990(4) |
| M−H(11) | 1.65(4) | | | | 1.95(2) | | | |
| B(11)−H(11) | 1.19(4) | | | | 1.08(2) | | | |
| Cent−M−C(Me) | | 153.40, 151.41 | 151.47 | 140.51 | | 138.58 | 130.30 | 148.11, 150.73 |
| Cent−M−N | | 103.37, 103.49 | 104.81 | 113.40 | | 118.20 | 125.64 | 110.07, 111.90 |
| C7−C12−N | 110.9(4) | 103.6(3) | 103.4(2) | 104.4(4) | | | | |
| B(11)−H(11)−M | 121.4(3) | | | | 94.7(1) | | | |
| N−M−C(Me) | 109.6(2), 112.3(3) | 103.1(2), 104.3(2) | 99.1(2) | 105.6(3) | 110.4(1), 112.2(1) | 99.1(2) | 118.0(2) | 98.8(3), 99.0(2) |

[a] Bond lengths in Å, angles in deg.

**Table 5.** Important Interatomic Distances (Å) and Angles (deg) for Compounds **3**, **5**, **6**, and **7**



| | 3 | 5[a] | 6 | 7 |
|---|---|---|---|---|
| Cent−M | | 1.713 | 1.703 | 1.862 |
| M−C15 | 1.910(5), 1.936(6) | 1.944(5) | 1.927(3) | 1.949(8) |
| M−N | 1.997(4) | 2.037(4) | 2.063(2) | 2.100(5) |
| Cent−M−C15 | | 152.41 | 151.47 | 161.14 |
| Cent−M−N (α−angle) | | 103.43 | 104.81 | 92.55 |
| Cent−C7−C12 | | 137.84 | 140.32 | 133.40 |
| C7−C12−N | 110.9(4) | 103.6(3) | 103.4(2) | 104.4(4) |
| N−M−C15 | 109.6(2), 112.3(3) | 103.7(2) | 103.4(1) | 105.6(3) |
| C12−N−M | 108.9(3) | 100.4(2) | 99.1(2) | 106.2(3) |
| C13−N−C14 | 108.5(4) | 108.8(4) | 107.0(3) | 108.2(5) |
| C13−N−M | 110.7(3) | 112.7(3) | 116.7(2) | 111.9(4) |
| C14−N−M | 110.8(3) | 112.4(3) | 110.5(2) | 108.2(4) |

[a] Average value.

**Table 6.** Important Interatomic Distances (Å) and Angles (deg) for Compounds **14**, **18**, **19**, and **23**



| | 14 | 18 | 19 | 23[a] |
|---|---|---|---|---|
| Cent−M | | 1.705 | 1.907 | 1.774 |
| M−C29 | 1.961(3), 1.965(3) | 1.935(5) | 1.961(4) | 1.926(6) |
| M−N | 2.066(2) | 2.075(4) | 2.138(3) | 1.990(4) |
| Cent−M−C29 | | 138.58 | 152.90 | 149.42 |
| Cent−M−N (α−angle) | | 118.20 | 103.85 | 110.99 |
| Cent−C7−C12 | | 154.44 | 148.37 | 151.44 |
| N−M−C29 | 110.4(1), 112.2(1) | 99.1(2) | 103.2(1) | 98.9(2) |
| C13−N−M | 109.2(2) | 111.1(3) | 118.0(2) | 117.0(3) |
| C14−N−C21 | 111.3(2) | 107.8(4) | 109.0(2) | |
| C14−N−M | 113.7(2) | 108.1(3) | 100.7(2) | 111.5(3) |
| C21−N−M | 105.6(2) | 109.9(3) | 109.4(2) | |

[a] Average value.

The Al-bound methyl group is directed over the boron atoms of the dicarbollide cage face due to the aluminum-coordinated NMe$_2$ sidearm. It is clear that the interactions between the apical aluminum and the boron with the C$_2$B$_3$ pentagonal face are weakened upon complexation with the NMe$_2$ sidearm. The tilt angles of the Al-bound methyl group from the Al−B10 and Al−C$_2$B$_3$ centroid axes are 113.56° and 152.41° (av), respectively.

As shown in Figure 4, the structure of aluminum complex **6** reveals that it is isomorphous and isostructural to **5**. The central aluminum atom is π-bound to the dicarbollyl fragment and σ-bound to the methylamine sidearm in a constrained manner. The centroid distance from the aluminum atom (1.703 Å) is smaller than that found in **5**, indicating that there are strong π-bonding interactions between Al$^{3+}$ and dicarbollide.[14] The methyl substituent on the carbon atom of the C$_2$B$_3$-pentagonal

face renders stronger interaction with the central aluminum. All other bond distances and angles around the aluminum and the nitrogen atoms are similar to those found in **5**. The structures of **5** and **6** reported here represent the first solid-state structural information on constrained-geometry aluminum complexes with $\eta^5$:$\eta^1$-mode coordination. These results were communicated recently.[15]

As shown in Figure 5, complex **7** serves as an example to outline the general characteristics of $\pi$,$\sigma$-bonded gallium CGCs. The central gallium atom is pseudotetrahedrally coordinated to the methyl ligand [Ga–C(Me), 1.949(8) Å], the NMe$_2$ sidearm [Ga–N, 2.100(5) Å], and the C$_2$B$_3$ plane of the dicarbollyl ligand [Ga–C$_2$B$_3$(centroid), 1.862 Å]. The Ga–N distance is consistent with a regular Ga–N($sp^3$) single bond[16] and confirms that the N-donor atom is coordinated to the metal in a strain-free manner. The C$_2$B$_3$ ligand is $\eta^5$-coordinated to the gallium metal center, but rather unsymmetrically with short Ga–B and long Ga–C distances.[12b,17] It is well-known that metallacarborane compounds containing the [$nido$-7,8-C$_2$B$_9$H$_{11}$]$^{2-}$ and [$nido$-2,3-C$_2$B$_4$H$_6$]$^{2-}$ ligands and their C-substituted derivatives may exhibit varying degrees of distortion from idealized closo geometry by undergoing a "slipping" of the capping metal across the C$_2$B$_3$ cage face in the direction of the apical boron atom.[14f] Thus, the Ga–B9/B10/B11 [2.236(8)/2.213(7)/2.313(6) Å] linkage is markedly shorter than the Ga–C7/C8 [2.546(5)/2.515(6) Å] linkage. The corresponding C$_2$B$_3$(centroid)–C7–C12 angle is 133.40°. The endocyclic C7–C12–N bond angle is 104.4(4)°, which is a departure from the tetrahedral $sp^3$-C value. In **7**, the $\alpha$-angle is 92.55°, which is markedly shorter than that found in **5**. In compound **7**, the direction of the Ga-bound methyl group is pointing toward the B10 atom of the C$_2$B$_3$ open face.

Another template system designed to stabilize $\pi$,$\sigma$-CGCs was the ethylene-bridged dicarbollyl/amine ligand system. However, evidence supporting the $\eta^1$:$\eta^1$-coordination of the dicarbollyl/ethylamino group to the aluminum atom in complex **14** is provided by X-ray crystal structure analysis. As shown in Figure 6, complex **14** is structurally related to **3** in the sense that it adopts $\eta^1$:$\eta^1$-type aluminum CGC with an ethylene spacer. Complex **14** constitutes a similar geometry found in $\sigma$,$\sigma$-type

bonding for [($\eta^1$-Cp*)(CH$_2$)$_2$($\eta^1$-NBn$_2$)]AlMe$_2$ **B**.[2b] The central aluminum atom is coordinated to the B11 atom and two methyl ligands in a $\sigma$-bonding fashion. The dibenzylamino fragment coordinates to the aluminum in the remaining basal site of the overall pseudotetrahedral conformation giving a six-membered B–Al–N–C–C–C ring. Selected bond lengths and angles for **14** are listed in Table 6 and in the Supporting Information. The Al–N bond length is 2.066(2) Å, which lies within the usual range for a dative bond between aluminum and nitrogen atoms.[13] Similar to **3**, the H11 atom at the B11 exhibits agostic interaction[12] with the aluminum metal. In general, metric parameters around the aluminum center are similar to those found in **3**.

Some general structural features for $\pi$,$\sigma$-CGCs with an ethylene spacer are compared in Table 6, where selected bond distances and angles are presented. Some of the general structural characteristics of $\pi$,$\sigma$-CGCs are discussed below by using selected example **18**. The X-ray crystal structure of **18** (Figure 7) revealed that the Al atom essentially adopts a half-metallocene type geometry, having an $\eta^5$-coordination with the dicarbollyl ligand and an $\eta^1$-coordination with the dibenzylamino tether and the methyl ligand. In **18**, the Al–C$_2$B$_3$ face (centroid) distance is 1.705 Å, and the Al–N distance is 2.075(4) Å. These values correlate well with those found in similar complexes **5** and **6** which have values of 1.713 (av)/1.703 Å for the Al–C$_2$B$_3$ face (centroid) distances and 2.037 (av) and 2.063(2) Å for the Al–N(amino) distances, respectively. Complex **18** shows similar bond angles and distances around the aluminum center to those found in **5** except a few bond angles including C$_2$B$_3$(centroid)–Al–C(Me) (138.58° vs 151.41°), C$_2$B$_3$(centroid)–Al–N (118.20° vs 103.43°), and C$_2$B$_3$(centroid)–C7–C12 (154.44° vs 137.84°). Such deviations are arisen due to the extended length of the ethylene spacer between the dicarbollyl and the benzyl amine functionalities. Similar to **5**, the Al-bound methyl group is directed over the B11 atom of the dicarbollide cage face.

The X-ray crystal structure of **19** (Figure 8) revealed that the Ga atom adopts an $\eta^5$-coordination with the dicarbollyl rings and an $\eta^1$-coordination with the dibenzylamino side groups. Overall, complex **19** adopts a half-metallocene type geometry, with two legs of methyl and dibenzylamine ligands. The Ga–N distance of 2.138(3) Å confirms that the N-donor atom is coordinated to the metal in a strain-free manner and the bond distance is consistent with a Ga–N($sp^3$) dative bond.[16] The noticeable lengthening, compared to **18**, of the Ga–C$_2$B$_3$-(centroid) distance (1.907 Å) and the $\eta^5$-coordination of **19** show an unsymmetrical linkage between the central gallium atom and carbon and boron atoms on the C$_2$B$_3$ open face. A significant bond length difference is noted when Ga–C7/C8 are compared with Ga–B9/B10/B11: average bond lengths of Ga–C7/C8 and Ga–B9/B10/B11 are 2.622 Å and 2.229 Å, respectively. As a result, the gallium atom occupies an apical vertex of an icosahedron and is slipped significantly toward the apical boron above the C$_2$B$_3$ face in an $\eta^3$-fashion.

The molecular structure of **23**, determined by X-ray diffraction, is shown in Figure 9. The crystal structure of **23** exhibits a strong resemblance to that found in **18**, showing two independent molecules in the asymmetric unit related by twofold symmetry. Structural analysis of **23** showed that the benzylamino group was intramolecularly coordinated to the aluminum atom. Therefore, the complex adopts an essentially "piano-stool" structure with the aluminum atom $\eta^5$-coordinated on one side by a dicarbollyl group and $\eta^1$-bonded to the other by the

(14) (a) Young, D. A. T.; Willey, G. R.; Hawthorne, M. F.; Churchill, M. R.; Reis, A. H., Jr *J. Am. Chem. Soc.* **1970**, *92*, 6663. (b) Churchill, M. R.; Reis, A. H.; Young, D. A.; Wiley, G. R.; Hawthorne, M. F. *J. Chem. Soc., Chem Commun.* **1971**, 298. (c) Churchill, M. R.; Reis, A. H. *J. Chem. Soc., Dalton Trans.* **1972**, 1317. (d) Rees, W. S., Jr.; Schubert, D. M.; Knobler, C. B.; Hawthorne, M. F. *J. Am. Chem. Soc.* **1986**, *108*, 5367. (e) Getman, T. D.; Shore, S. G. *Inorg. Chem.* **1988**, *27*, 3439. (f) Schubert, D. M.; Bandman, M. A.; Rees, W. S., Jr.; Knobler, C. B.; Lu, P.; Nam, W.; Hawthorne, M. F. *Organometallics* **1990**, *9*, 2046.

(15) Son, K.-C.; Lee, Y.-J.; Cheong, M.; Ko, J.; Kang, S. O. *J. Am. Chem. Soc.* **2006**, *128*, 12086.

(16) (a) Andrews, P. C.; Gardiner, M. G.; Raston, C. L.; Tolhurst, V.-A. *Inorg. Chim. Acta* **1997**, *259*, 249. (b) Hosmane, N. S.; Lu, K. J.; Zhang, H.; Maguire, J. A. *Organometallics* **1997**, *16*, 5163. (c) Lee, J. -D.; Baek, C.-K.; Ko, J.; Park, K.; Cho, S.; Min, S. -K.; Kang, S. O. *Organometallics* **1999**, *18*, 2189. (d) Bensiek, S.; Bangel, M.; Neumann, B.; Stammler, H. -G.; Jutzi, P. *Organometallics* **2000**, *19*, 1292. (e) Tian, X.; Fröhlich, R.; Pape, T.; Mitzel, N. W. *Organometallics* **2005**, *24*, 5294.

(17) (a) Grimes, R. N.; Rademaker, W. J. *J. Am. Chem. Soc.* **1969**, *91*, 6498. (b) Grimes, R. N.; Rademaker, W. J.; Denniston, M. L.; Bryan, R. F.; Greene, P. T. *J. Am. Chem. Soc.* **1972**, *94*, 1865. (c) Hosmane, N. S.; Lu, K.-J.; Zhang, H.; Jia, L. *Organometallics* **1991**, *10*, 963. (d) Saxena, A. K.; Maguire, J. A.; Hosmane, N. S. *Chem. Rev.* **1997**, *97*, 2421. (e) Hosmane, N. S. *J. Organomet. Chem.* **1999**, *581*, 13.

(18) (a) *SMART* and *SAINT*; Bruker Analytical X-ray Division: Madison, WI, 2002. (b) Sheldrick, G. M. *SHELXTL-PLUS Software Package*; Bruker Analytical X-ray Division: Madison, WI, 2002.

**Chart 2.** Optimized Structures of Aluminum π,σ-CGC Complex **5**
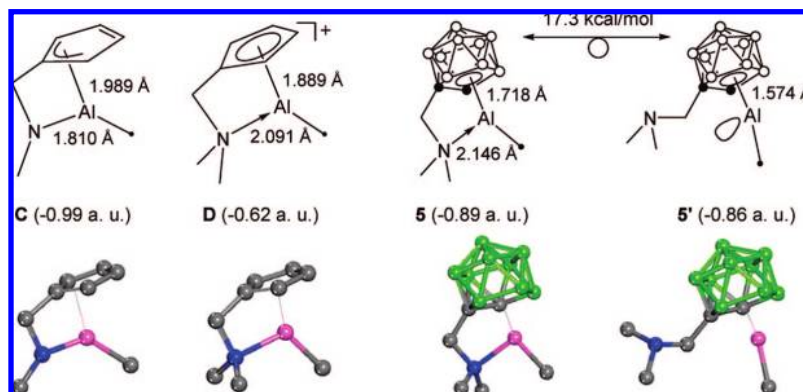


benzylamino group and one methyl ligand. The Al−C$_2$B$_3$(centroid) bond length in **23** is 1.774 Å (av). The Al−N bond is shorter [1.990(4) Å (av)] than that found in analogue **18** [2.075(4) Å]. The shorter Al−N distance is due to the reduction of steric congestion around the nitrogen atom by replacing one benzyl group with a hydrogen atom.

**DFT Calculation.** To understand the bonding interactions between the aluminum ion and dicarbollyl ligand, relativistic density functional theory (DFT) calculations using the Amsterdam density functional (ADF) code with the Becke and Perdew functional were performed on model complexes such as [(η$^3$-Cp)CH$_2$(η$^1$-NMe)]Al(Me) **C**, [{(η$^5$-Cp)CH$_2$(η$^1$-NMe$_2$)}-Al(Me)]$^{+1}$ **D**, and [(η$^5$-C$_2$B$_9$)CH$_2$(η$^1$-NMe$_2$)]Al(Me) **5** (Chart 2). We first concentrated on the simplest model compound, the Cp-amido complex (**C**), the Lewis acid−base adduct between AlMe$^{+2}$ and [(Cp)CH$_2$(NMe)]$^{-2}$. We then examined the effect of adding a methyl substituent to the nitrogen atom and compensating the charge with +1 as shown in the Cp-amino complex **D**, the Lewis acid−base adduct between AlMe$^{+2}$ and [(Cp)CH$_2$(NMe$_2$)]$^{-1}$. Adding a methyl substituent to the nitrogen changes the hapticity of the Cp ring from η$^3$ to η$^5$ and the bond distance of Al−N from 1.810 Å to 2.091 Å. These changes occur because the two lone pairs on the amido-nitrogen atom in **C** donate electrons more efficiently than the single lone pair on the amino-nitrogen atom in **D**. This effect is partly compensated in **D** by the aluminum atom accepting more electron density from the Cp ring. In **D**, the calculated energy shows a preference for π,σ-bonding, consistent with the results of the DFT calculation previously performed on the related complex, [(η$^5$-Cp)H$_2$Si(η$^1$-NMe)}Al]$^{+1}$.[2c]

Fixing the nitrogen part in **D** and changing the Cp ring to an isolobal dicarbollyl moiety as in **5** further increase the Al−N bond distance from 2.091 to 2.146 Å. The relative formation enthalpy of the Lewis acid−base adduct **5** (−0.89 au) is compared with that of **C** (−0.99 au) and **D** (−0.62 au) in Chart 2. The results indicate that complex **5** is less stable than **C**, reverting to an η$^5$:η$^1$-bonding which was authenticated in a structural study of **5**. This is consistent with the fact that the σ-bonding interaction between Al and N in **C** is stronger than that in **D** and the π-bonding interaction between the dicarbollyl unit and Al in **5** is stronger than that between Cp and Al in **D**.

A strong π-type interaction between aluminum and the dicarbollyl unit was clearly demonstrated by the DFT calculation in which the untethered structure of **5′** was optimized. The existence of a half-sandwich aluminum complex of **5′** is further confirmed by a variable temperature NMR study of **6** (Figure S9 in the Supporting Information). Detachment of the tethered

amine sidearm from the aluminum center ensures the stability of η$^5$-type coordination with the dicarbollyl ligand. Thus, introduction of the dicarbollyl unit onto the ring stabilizes the π,σ-type bonding mode, which was not found for the complex [(η$^1$-Cp*)Me$_2$Si(η$^1$-N$^t$Bu)]Al(Me)(THF) **A**. We believe that both the σ-electronic contribution from the amine sidearm and the π-bonding capability of the dicarbollyl unit create an ideal bonding environment for the formation of novel constrained-geometry aluminum complexes.

It has been also noted that preference for π,σ-type bonding of the aluminum atom is dependent on the tether length of dicarbollylamines. As shown in Scheme 1 and 3, a methylene tether favors the formation of π,σ-type bonding, whereas an ethylene surrogate yields only σ,σ-type bonding. Although σ,σ-type bonding was dominant even in the case of a methylene tether in a short reaction time, it will be eventually converted to π,σ-type bonding in a prolonged reaction as shown in Scheme 1. To gain insight on which ligand system is well suited for a π,σ-bonding interaction, energy profiles for the transformation of the σ,σ- to π,σ-bonded structure were studied by means of DFT calculations. (Figure 10) Complexes **3** and **14** were taken as prototype examples of σ,σ-type bonding for a methylene- and ethylene-tethered dicarbollylamine ligand, respectively. As shown in Figure 11, transition states from each ligand leading to a π,σ-bonded structure comprise a similar structural motif, having significant interactions between three atoms: the aluminum, the carbon of the methyl, and the bridging hydrogen. Such interactions eventually allow elimination of methane to form desired π,σ-bonded structures. Activation energies required for each transition state of the methylene and ethylene tethers are 29.5 and 28.6 kcal/mol, respectively. Further calculations on each π,σ-bonded structure **5** and **18** were carried out and revealed that the π,σ-bonded structure **5** is more stable than that of **18** by 3.1 kcal/mol. Although a slightly higher activation energy is required for the methylene tether, the energy gain by forming a π,σ-bonded structure is excessive.

## Summary

Herein, we report for the first time the structural characterization of the constrained-geometry group 13 main group metal complexes with π,σ-bonding interaction and an explanation of the preference for the π,σ-bonded constrained geometry in dicarbollylamine ligand systems based on DFT calculations. Thus, we found that (1) dicarbollyl and amine functional groups are essential for the formation of the π,σ-type bonded structure; (2) a methyl substituent on the C8 atom of the dicarbollyl open face renders a stronger π-type interaction of the metal atom
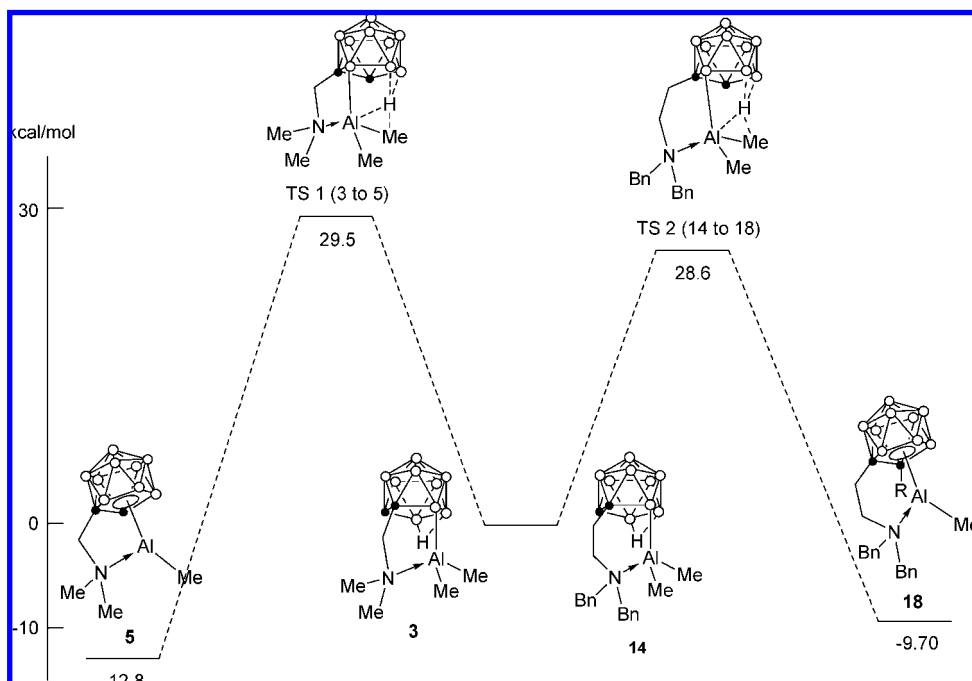
**Figure 10.** Energy profile of transitions from $\sigma,\sigma$-type to $\pi,\sigma$-type bonding for methylene- and ethylene-bridged dicarbollylamine systems **3** and **14**.
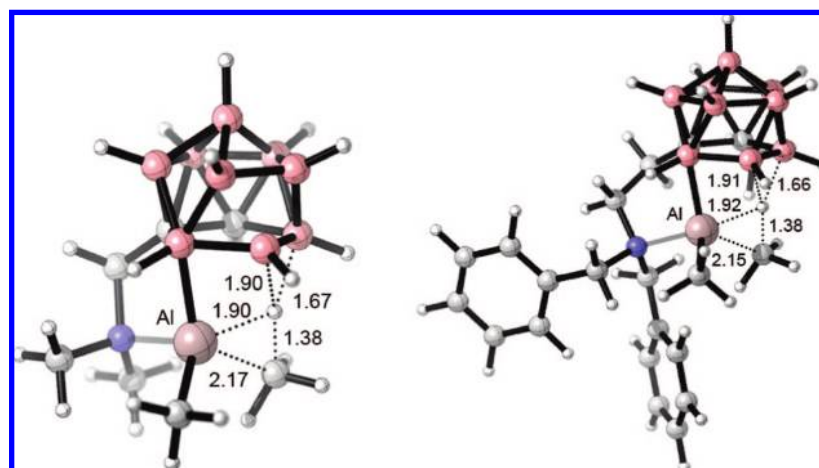


**Figure 11.** Transition states of methylene- (TS 1) and ethylene-bridged (TS 2) dicarbollylamino aluminum complexes.

with dicarbollyl unit; (3) in the case of dicarbollyl-methylene-amine combined with the aluminum atom, a stepwise transformation from $\sigma,\sigma$- to $\pi,\sigma$-type bonding interaction was noted, revealing $\sigma,\sigma$-bonded structure is, indeed, a kinetic product; (4) preference for each $\sigma,\sigma$- and $\pi,\sigma$-type bonding interaction comes with the choice of the length of the bridging unit, in which the methylene bridge favors $\pi,\sigma$-bonding, while ethylene spacer stabilizes $\sigma,\sigma$-bonding interaction; and (5) heavier congeners, such as the gallium and indium atoms, favor the formation of the $\pi,\sigma$-bonded structure regardless of tether units.

## Experimental Section

**General Procedures.** All manipulations were performed under a dry, oxygen-free nitrogen or argon atmosphere using standard Schlenk techniques or in a vacuum atmosphere HE-493 drybox. Toluene was distilled under nitrogen from sodium/benzophenone. Benzene-$d_6$ and toluene-$d_8$ were distilled under nitrogen from sodium and stored in a Schlenk storage flask until needed. AlMe$_3$, GaMe$_3$, and InMe$_3$ were used as received from Strem Chemical.

*o*-Carborane was purchased from KatChem and used after sublimation. The starting materials **1**, **2**, **11**, and **12** were synthesized according to literature procedures.[10,11] $^1$H, $^{11}$B, and $^{13}$C NMR spectra were recorded on a Varian Mercury 300 spectrometer operating at 300.1, 96.3, and 75.4 MHz, respectively. All $^{11}$B chemical shifts were referenced to BF$_3$·O(C$_2$H$_5$)$_2$ (0.0 ppm) with a negative sign indicating an upfield shift. All proton and carbon chemical shifts were measured relative to internal residual peaks from the lock solvent (99.5% C$_6$D$_6$, 99.5% CD$_3$C$_6$D$_5$) and then referenced to Me$_4$Si (0.00 ppm). IR spectra were recorded on a Biorad FTS-165 spectrophotometer. Elemental analyses were performed with a Carlo Erba Instruments CHNS-O EA1108 analyzer. All melting points were uncorrected. High-resolution mass spectra were measured at the Korea Basic Science Institute.

**Preparation of [($\eta^1$-RC$_2$B$_9$H$_{10}$)CH$_2$($\eta^1$-NMe$_2$)]AlMe$_2$ (R = H 3, Me 4).** To a stirred 20 mL aliquot of a toluene solution containing **1** (0.19 g, 1.0 mmol) was added a 5 mL aliquot of a toluene solution of AlMe$_3$ (0.09 g, 1.2 mmol) by cannula at −78 °C. After addition was complete, the cold bath was removed and the solution was refluxed under N$_2$ for 30 min. The formation of **3**

was demonstrated by $^1$H NMR spectroscopy. Volatiles were removed under vacuum, and the residue was purified by recrystallization with toluene at −15 °C. **3**: Yield: 0.20 g (81%). Mp: 137 °C (dec.). HRMS: Calcd for $[^{12}C_7{}^{11}B_9{}^1H_{25}{}^{14}N^{27}Al]^+$: 249.2640. Found: 249.2650. IR spectrum (KBr pellet, cm$^{-1}$) $\nu$(B−H) 2537, $\nu$(C−H) 3107, 3115. $^1$H NMR (300 MHz, CD$_3$C$_6$D$_5$) δ −3.20 (br, 1H, B−*H*−B), −0.53 (s, 3H, Al*Me*), −0.17 (s, 3H, Al*Me*), 1.49 (s, 3H, CH$_2$N*Me*$_2$), 1.74 (s, 3H, CH$_2$N*Me*$_2$), 1.92 (s, 1H, C$_{cab}$*H*), 2.27 (d, 1H, $^2J_{HH}$ = 15 Hz, C*H*$_2$NMe$_2$), 2.59 (d, 1H, $^2J_{HH}$ = 15 Hz, C*H*$_2$NMe$_2$). $^{11}$B NMR (96.3 MHz, CD$_3$C$_6$D$_5$) δ −8.82 (1B), −14.91 (1B), −22.39 (2B), −24.55 (2B), −30.85 (2B), −38.83 (1B).

**4**: A procedure analogous to that used to prepare **3** was used, but starting from the zwitterion **2** (0.21 g, 1.0 mmol). Yield: 0.21 g (80%). Mp: 133 °C (dec.). HRMS: Calcd for $[^{12}C_8{}^{11}B_9{}^1H_{27}{}^{14}N^{27}Al]^+$: 263.2796. Found: 263.2792. IR spectrum (KBr pellet, cm$^{-1}$) $\nu$(B−H) 2539, $\nu$(C−H) 3112, 3125. $^1$H NMR (300 MHz, CD$_3$C$_6$D$_5$) δ −3.03 (br, 1H, B−*H*−B), −0.39 (s, 3H, Al*Me*), −0.20 (s, 3H, Al*Me*), 1.66 (s, 3H, CH$_2$N*Me*$_2$), 1.81 (s, 3H, C$_{cab}$*Me*), 1.84 (s, 3H, CH$_2$N*Me*$_2$), 2.46 (d, 1H, $^2J_{HH}$ = 15 Hz, C*H*$_2$NMe$_2$), 2.68 (d, 1H, $^2J_{HH}$ = 15 Hz, C*H*$_2$NMe$_2$). $^{11}$B NMR (96.3 MHz, CD$_3$C$_6$D$_5$) δ −11.16 (2B), −18.76 (1B), −20.64 (1B), −26.15 (2B), −28.89 (1B), −31.89 (1B), −38.31 (1B).

**Preparation of $[(\eta^5$-RC$_2$B$_9$H$_9$)CH$_2(\eta^1$-NMe$_2$)]AlMe (R = H 5, Me 6).** To a stirred 20 mL aliquot of a toluene solution containing **1** (0.19 g, 1.0 mmol) was added a 5 mL aliquot of a toluene solution of AlMe$_3$ (0.09 g, 1.2 mmol) by cannula at −78 °C. After addition was complete, the cold bath was removed and the solution was refluxed under N$_2$ for 10 h. The formation of **5** was demonstrated by $^1$H NMR spectroscopy. The volatiles were removed under vacuum, and the residue was purified by recrystallization with toluene at −15 °C. **5**: Yield: 0.19 g (82%). Mp: 155 °C (dec.). HRMS: Calcd for $[^{12}C_6{}^{11}B_9{}^1H_{21}{}^{14}N^{27}Al]^+$: 233.2327. Found: 233.2319. IR spectrum (KBr pellet, cm$^{-1}$) $\nu$(B−H) 2538, $\nu$(C−H) 3109, 3192. $^1$H NMR (300 MHz, C$_6$D$_6$) δ −0.19 (s, 3H, Al*Me*), 1.34 (s, 3H, CH$_2$N*Me*$_2$), 1.64 (s, 3H, CH$_2$N*Me*$_2$), 1.72 (d, 1H, $^2J_{HH}$ = 16 Hz, C*H*$_2$NMe$_2$), 1.78 (s, 1H, C$_{cab}$*H*), 2.05 (d, 1H, $^2J_{HH}$ = 16 Hz, C*H*$_2$NMe$_2$). $^{11}$B NMR (96.3 MHz, C$_6$D$_6$) δ −13.29 (1B), −19.52 (2B), −24.45 (3B), −27.78 (2B), −34.69 (1B).

**6**: A procedure analogous to that used to prepare **5** was used, but starting from the zwitterions **2** (0.21 g, 1.0 mmol). Yield: 0.20 g (81%). Mp: 161 °C (dec.). HRMS: Calcd for $[^{12}C_7{}^{11}B_9{}^1H_{23}{}^{14}N^{27}Al]^+$: 247.2483. Found: 247.2494. IR spectrum (KBr pellet, cm$^{-1}$) $\nu$(B−H) 2542, $\nu$(C−H) 2874, 2932, 2966, 3035. $^1$H NMR (300 MHz, C$_6$D$_6$) δ −0.21 (s, 3H, Al*Me*), 1.33 (s, 3H, C$_{cab}$*Me*), 1.48 (s, 3H, CH$_2$N*Me*$_2$), 1.84 (s, 3H, CH$_2$N*Me*$_2$), 1.97 (d, 1H, $^2J_{HH}$ = 14 Hz, C*H*$_2$NMe$_2$), 2.17 (d, 1H, $^2J_{HH}$ = 14 Hz, C*H*$_2$NMe$_2$). $^{11}$B NMR (96.3 MHz, C$_6$D$_6$) δ −12.00 (1B), −15.77 (1B), −18.34 (2B), −20.22 (3B), −27.26 (1B), −34.28 (1B).

**Preparation of $[(\eta^5$-RC$_2$B$_9$H$_9$)CH$_2(\eta^1$-NMe$_2$)]GaMe (R = H 7, Me 8).** To a stirred 20 mL aliquot of a toluene solution containing **1** (0.19 g, 1.0 mmol) was added a 5 mL aliquot of a toluene solution of GaMe$_3$ (0.13 g, 1.1 mmol) by cannula at −78 °C. After addition was complete, the cold bath was removed and the solution was refluxed under N$_2$ for 36 h. The formation of **7** was demonstrated by $^1$H NMR spectroscopy. The solvent was then removed under vacuum, and the residue was purified by recrystallization with toluene at −15 °C. **7**: Yield: 0.21 g (77%). Mp: 148 °C (dec.). HRMS: Calcd for $[^{12}C_6{}^{11}B_9{}^1H_{21}{}^{14}N^{70}Ga]^+$: 275.1767. Found: 275.1773. IR spectrum (KBr pellet, cm$^{-1}$) $\nu$(B−H) 2536, $\nu$(C−H) 3102, 3135. $^1$H NMR (300 MHz, CD$_3$C$_6$D$_5$) δ 0.42 (s, 3H, Ga*Me*), 1.64 (s, 3H, CH$_2$N*Me*$_2$), 1.85 (d, 1H, $^2J_{HH}$ = 14 Hz, C*H*$_2$NMe$_2$), 1.87 (s, 3H, CH$_2$N*Me*$_2$), 2.06 (s, 1H, C$_{cab}$*H*), 2.23 (d, 1H, $^2J_{HH}$ = 14 Hz, C*H*$_2$NMe$_2$). $^{11}$B NMR (96.3 MHz, CD$_3$C$_6$D$_5$) δ −13.19 (1B), −17.45 (1B), −20.20 (3B), −21.54 (1B), −27.30 (1B), −33.73 (2B).

**8**: A procedure analogous to that used to prepare **7** was used, but starting from the zwitterions **2** (0.21 g, 1.0 mmol). Yield: 0.19 g (66%). Mp: 143 °C (dec.). HRMS: Calcd for $[^{12}C_7{}^{11}B_9{}^1H_{23}{}^{14}N^{70}Ga]^+$:

289.1924. Found: 289.1934. IR spectrum (KBr pellet, cm$^{-1}$) $\nu$(B−H) 2516, $\nu$(C−H) 3037, 3107. $^1$H NMR (300 MHz, CD$_3$C$_6$D$_5$) δ 0.38 (s, 3H, Ga*Me*), 1.53 (s, 3H, C$_{cab}$*Me*), 1.75 (s, 3H, CH$_2$N*Me*$_2$), 1.89 (d, 1H, $^2J_{HH}$ = 14 Hz, C*H*$_2$NMe$_2$), 2.02 (s, 3H, CH$_2$N*Me*$_2$), 2.24 (d, 1H, $^2J_{HH}$ = 14 Hz, C*H*$_2$NMe$_2$). $^{11}$B NMR (96.3 MHz, CD$_3$C$_6$D$_5$) δ −12.46 (1B), −15.81 (2B), −17.17 (1B), −20.53 (3B), −33.44 (2B).

**Preparation of $[(\eta^5$-RC$_2$B$_9$H$_9$)CH$_2(\eta^1$-NMe$_2$)]InMe (R = H 9, Me 10).** To a stirred 20 mL aliquot of a toluene solution containing **1** (0.19 g, 1.0 mmol) was added a 5 mL aliquot of a toluene solution of InMe$_3$ (0.16 g, 1.0 mmol) by cannula at −78 °C. After addition was complete, the cold bath was removed and the solution was refluxed under N$_2$ for 2 h. The formation of **9** was demonstrated by $^1$H NMR spectroscopy. The solvent was then removed under vacuum, and the residue was purified by recrystallization with toluene at −15 °C. **9**: Yield: 0.19 g (72%). Mp: 144 °C (dec.). HRMS: Calcd for $[^{12}C_6{}^{11}B_9{}^1H_{21}{}^{14}N^{115}In]^+$: 321.1550. Found: 321.1564. IR spectrum (KBr pellet, cm$^{-1}$) $\nu$(B−H) 2523, $\nu$(C−H) 3064, 3167. $^1$H NMR (300 MHz, CD$_3$C$_6$D$_5$) δ 0.11 (s, 3H, In*Me*), 1.42 (s, 3H, CH$_2$N*Me*$_2$), 1.70 (s, 3H, CH$_2$N*Me*$_2$), 1.80 (s, 1H, C$_{cab}$*H*), 2.00 (d, 1H, $^2J_{HH}$ = 13 Hz, C*H*$_2$NMe$_2$), 2.17 (d, 1H, $^2J_{HH}$ = 13 Hz, C*H*$_2$NMe$_2$). $^{11}$B NMR (96.3 MHz, CD$_3$C$_6$D$_5$) δ −16.05 (1B), −18.71 (1B), −20.36 (2B), −22.04 (1B), −27.03 (3B), −36.13 (1B).

**10**: A procedure analogous to that used to prepare **9** was used, but starting from the zwitterions **2** (0.21 g, 1.0 mmol). Yield: 0.19 g (66%). Mp: 141 °C (dec.). HRMS: Calcd for $[^{12}C_7{}^{11}B_9{}^1H_{23}{}^{14}N^{115}In]^+$: 335.1707. Found: 335.1718. IR spectrum (KBr pellet, cm$^{-1}$) $\nu$(B−H) 2519, $\nu$(C−H) 3028, 3143. $^1$H NMR (300 MHz, CD$_3$C$_6$D$_5$) δ 0.45 (s, 3H, In*Me*), 1.51 (s, 3H, C$_{cab}$*Me*), 1.82 (s, 3H, CH$_2$N*Me*$_2$), 1.90 (d, 1H, $^2J_{HH}$ = 13 Hz, C*H*$_2$NMe$_2$), 1.94 (s, 3H, CH$_2$N*Me*$_2$), 2.18 (d, 1H, $^2J_{HH}$ = 13 Hz, C*H*$_2$NMe$_2$). $^{11}$B NMR (96.3 MHz, CD$_3$C$_6$D$_5$) δ −12.23 (1B), −18.97 (3B), −20.97 (1B), −22.38 (2B), −29.06 (1B), −34.12 (1B).

**Preparation of $[(\eta^1$-RC$_2$B$_9$H$_{10}$)CH$_2$CH$_2(\eta^1$-NBn$_2$)]AlMe$_2$ (R = H 13, Me 14).** To a stirred 20 mL aliquot of a toluene solution containing **11** (0.36 g, 1.0 mmol) was added a 5 mL aliquot of a toluene solution of AlMe$_3$ (0.09 g, 1.2 mmol) by cannula at −78 °C. After addition was complete, the cold bath was removed and the solution was refluxed under N$_2$ for 12 h. The formation of **5** was demonstrated by $^1$H NMR spectroscopy. The solvent was removed *in vacuo*, and the residue was purified by recrystallization with toluene at −15 °C. **13**: Yield: 0.33 g (80%). Mp: 143 °C (dec.). HRMS: Calcd for $[^{12}C_{20}{}^{11}B_9{}^1H_{35}{}^{14}N^{27}Al]^+$: 415.3422. Found: 415.3442. IR spectrum (KBr pellet, cm$^{-1}$) $\nu$(B−H) 2531, $\nu$(C−H) 3043, 3162. $^1$H NMR (300 MHz, CD$_3$C$_6$D$_5$) δ −3.31 (s, 1H, B−*H*−B), −0.47 (s, 3H, Al*Me*), −0.12 (s, 3H, Al*Me*), 1.85 (s, 1H, C$_{cab}$*H*), 1.88 (m, 1H, C*H*$_2$CH$_2$N), 2.17 (m, 1H, C*H*$_2$CH$_2$N), 3.51 (d, 2H, $^2J_{HH}$ = 14 Hz, NC*H*$_2$Ph), 3.73 (m, 1H, CH$_2$C*H*$_2$N), 3.80 (d, 2H, $^2J_{HH}$ = 14 Hz, NC*H*$_2$Ph), 4.23 (m, 1H, CH$_2$C*H*$_2$N), 7.24−7.36 (m, 10H, NCH$_2$*Ph*). $^{11}$B NMR (96.3 MHz, CD$_3$C$_6$D$_5$) δ −11.45 (3B), −14.29 (2B), −28.52 (2B), −39.62 (1B), −48.92 (1B).

**14**: A procedure analogous to that used to prepare **13** was used, but starting from the zwitterions **12** (0.37 g, 1.0 mmol). Yield: 0.34 g (80%). Mp: 141 °C (dec.). HRMS: Calcd for $[^{12}C_{21}{}^{11}B_9{}^1H_{37}{}^{14}N^{27}Al]^+$: 429.3567. Found: 429.3567. IR spectrum (KBr pellet, cm$^{-1}$) $\nu$(B−H) 2532, $\nu$(C−H) 3019, 3107. $^1$H NMR (300 MHz, CD$_3$C$_6$D$_5$) δ −3.08 (s, 1H, B−*H*−B), −0.45 (s, 3H, Al*Me*), −0.24 (s, 3H, Al*Me*), 1.57 (s, 3H, C$_{cab}$*Me*), 1.90 (m, 1H, C*H*$_2$CH$_2$N), 2.22 (m, 1H, C*H*$_2$CH$_2$N), 3.54 (d, 2H, $^2J_{HH}$ = 13 Hz, NC*H*$_2$Ph), 3.67 (m, 1H, CH$_2$C*H*$_2$N), 3.82 (d, 2H, $^2J_{HH}$ = 13 Hz, NC*H*$_2$Ph), 4.18 (m, 1H, CH$_2$C*H*$_2$N), 7.27−7.35 (m, 10H, NCH$_2$*Ph*). $^{11}$B NMR (96.3 MHz, CD$_3$C$_5$D$_6$) δ −13.11 (1B), −16.83 (2B), −20.48 (2B), −28.39 (1B), −38.54 (1B), −40.67 (1B), −44.55 (1B).

**Preparation of $[(\eta^5$-RC$_2$B$_9$H$_9$)CH$_2$CH$_2(\eta^1$-NBn$_2$)]AlMe (R = H 17, Me 18).** To a stirred 20 mL aliquot of a toluene solution containing **15** (0.49 g, 1.0 mmol) was added a 5 mL aliquot of a toluene solution of AlMe$_3$ (0.09 g, 1.2 mmol) by cannula at −78

°C. After addition was complete, the cold bath was removed and the solution was stirred for 1 h at room temperature. The formation of **17** was demonstrated by $^1$H NMR spectroscopy. The solvent was removed *in vacuo*, and the residue was purified by recrystallization with a toluene at −15 °C. **17**: Yield: 0.26 g (66%). Mp: 146 °C (dec.). HRMS: Calcd for $[^{12}C_{19}{}^{11}B_9{}^1H_{31}{}^{14}N^{27}Al]^+$: 399.3109. Found: 399.3092. IR spectrum (KBr pellet, cm$^{-1}$) $\nu$(B−H) 2520, $\nu$(C−H) 3013, 3067. $^1$H NMR (300 MHz, CD$_3$C$_6$D$_5$) $\delta$ −0.23 (s, 3H, Al*Me*), 1.98 (m, 1H, C*H*$_2$CH$_2$N), 2.01 (s, 1H, C$_{cab}$*H*), 2.14 (m, 1H, C*H*$_2$CH$_2$N), 3.40 (d, 2H, $^2J_{HH}$ = 15 Hz, NC*H*$_2$Ph), 3.58 (m, 1H, CH$_2$C*H*$_2$N), 3.80 (d, 2H, $^2J_{HH}$ = 15 Hz, NC*H*$_2$Ph), 4.20 (m, 1H, CH$_2$C*H*$_2$N), 7.34−7.45 (m, 10H, NCH$_2$*Ph*). $^{11}$B NMR (96.3 MHz, CD$_3$C$_5$D$_6$) $\delta$ −15.92 (2B), −17.38 (1B), −23.56 (1B), −26.55 (2B), −39.58 (1B), −41.52 (1B), −46.74 (1B).

**18**: A procedure analogous to that used to prepare **17** was used, but starting from the complex **16** (0.51 g, 1.0 mmol). Yield: 0.28 g (68%). Mp: 149 °C (dec.). HRMS: Calcd for $[^{12}C_{20}{}^{11}B_9{}^1H_{33}{}^{14}N^{27}Al]^+$: 413.3266. Found: 413.3252. IR spectrum (KBr pellet, cm$^{-1}$) $\nu$(B−H) 2523, $\nu$(C−H) 3054, 3097, 3125. $^1$H NMR (300 MHz, CD$_3$C$_6$D$_5$) $\delta$ −0.30 (s, 3H, Al*Me*), 1.63 (s, 3H, C$_{cab}$*Me*), 2.04 (m, 1H, C*H*$_2$CH$_2$N), 2.27 (m, 1H, C*H*$_2$CH$_2$N), 3.47 (d, 2H, $^2J_{HH}$ = 15 Hz, NC*H*$_2$Ph), 3.65 (m, 1H, CH$_2$C*H*$_2$N), 3.77 (d, 2H, $^2J_{HH}$ = 15 Hz, NC*H*$_2$Ph), 4.27 (m, 1H, CH$_2$C*H*$_2$N), 7.36−7.48 (m, 10H, NCH$_2$*Ph*). $^{11}$B NMR (96.3 MHz, CD$_3$C$_6$D$_5$) $\delta$ −17.37 (2B), −19.67 (2B), −24.19 (2B), −26.69 (1B), −40.37 (1B), −44.63 (1B).

**Preparation of [($\eta^5$-RC$_2$B$_9$H$_9$)CH$_2$CH$_2$($\eta^1$-NBn$_2$)]GaMe (R = H 19, Me 20).** To a stirred 20 mL aliquot of a toluene solution containing **11** (0.36 g, 1.0 mmol) was added a 5 mL aliquot of a toluene solution of GaMe$_3$ (0.12 g, 1.1 mmol) by cannula at −78 °C. After addition was complete, the cold bath was removed and the solution was refluxed under N$_2$ for 12 h. The formation of **19** was demonstrated by $^1$H NMR spectroscopy. Toluene was removed *in vacuo*, and the residue purified by recrystallization with a toluene at −15 °C. **19**: Yield: 0.33 g (75%). Mp: 152 °C (dec.). HRMS: Calcd for $[^{12}C_{19}{}^{11}B_9{}^1H_{31}{}^{14}N^{70}Ga]^+$: 441.2550. Found: 441.2538. IR spectrum (KBr pellet, cm$^{-1}$) $\nu$(B−H) 2532, $\nu$(C−H) 2954, 3063, 3117. $^1$H NMR (300 MHz, CD$_3$C$_6$D$_5$) $\delta$ 0.39 (s, 3H, Ga*Me*), 1.79 (s, 1H, C$_{cab}$*H*), 2.08 (m, 1H, C*H*$_2$CH$_2$N), 2.17 (m, 1H, C*H*$_2$CH$_2$N), 3.41 (d, 2H, $^2J_{HH}$ = 13 Hz, NC*H*$_2$Ph), 3.59 (m, 1H, CH$_2$C*H*$_2$N), 3.69 (d, 2H, $^2J_{HH}$ = 13 Hz, NC*H*$_2$Ph), 4.18 (m, 1H, CH$_2$C*H*$_2$N), 7.35−7.43 (m, 10H, NCH$_2$*Ph*). $^{11}$B NMR (96.3 MHz, CD$_3$C$_6$D$_5$) $\delta$ −12.97 (3B), −23.54 (2B), −27.18 (2B), −40.35 (1B), −44.27 (1B).

**20**: A procedure analogous to that used to prepare **19** was used, but starting from the complex **12** (0.37 g, 1.0 mmol). Yield: 0.34 g (75%). Mp: 155 °C (dec.). HRMS: Calcd for $[^{12}C_{20}{}^{11}B_9{}^1H_{33}{}^{14}N^{70}Ga]^+$: 455.2706. Found: 455.2686. IR spectrum (KBr pellet, cm$^{-1}$) $\nu$(B−H) 2511, $\nu$(C−H) 3062, 3097. $^1$H NMR (300 MHz, CD$_3$C$_6$D$_5$) $\delta$ 0.32 (s, 3H, Ga*Me*), 1.45 (s, 3H, C$_{cab}$*Me*), 2.01 (m, 1H, C*H*$_2$CH$_2$N), 2.23 (m, 1H, C*H*$_2$CH$_2$N), 3.44 (d, 2H, $^2J_{HH}$ = 13 Hz, NC*H*$_2$Ph), 3.68 (m, 1H, CH$_2$C*H*$_2$N), 3.78 (d, 2H, $^2J_{HH}$ = 13 Hz, NC*H*$_2$Ph), 4.24 (m, 1H, CH$_2$C*H*$_2$N), 7.36−7.46 (m, 10H, NCH$_2$*Ph*). $^{11}$B NMR (96.3 MHz, CD$_3$C$_6$D$_5$) $\delta$ −10.85 (1B), −12.27 (1B), −21.63 (3B), −31.06 (1B), −38.19 (2B), −44.66 (1B).

**Preparation of [($\eta^5$-RC$_2$B$_9$H$_9$)CH$_2$CH$_2$($\eta^1$-NHBn)]AlMe (R = H 23, Me 24).** To a stirred 20 mL aliquot of a toluene solution containing **21** (0.27 g, 1.0 mmol) was added a 5 mL aliquot of a toluene solution of AlMe$_3$ (0.09 g, 1.2 mmol) by cannula at −78 °C. After addition was complete, the cold bath was removed and the solution was refluxed under N$_2$ for 12 h. The formation of **23** was demonstrated by $^1$H NMR spectroscopy. Toluene was removed *in vacuo*, and the residue was purified by recrystallization with a toluene at −15 °C. **23**: Yield: 0.23 g (80%). Mp: 146 °C (dec.). HRMS: Calcd for $[^{12}C_{12}{}^{11}B_9{}^1H_{25}{}^{14}N^{27}Al]^+$: 309.2640. Found: 309.2649. IR spectrum (KBr pellet, cm$^{-1}$) $\nu$(B−H) 2532, $\nu$(C−H) 2912, 3036. $^1$H NMR (300 MHz, CD$_3$C$_6$D$_5$) $\delta$ −0.34 (s, 3H, Al*Me*), 2.12 (s, 1H, C$_{cab}$*H*), 2.07 (m, 1H, C*H*$_2$CH$_2$NH), 2.44 (m, 1H, C*H*$_2$CH$_2$NH), 3.38 (m, 1H, HNC*H*$_2$Ph), 3.57 (m, 1H, CH$_2$C*H*$_2$NH), 3.66 (m, 1H, HNC*H*$_2$Ph), 4.19 (m, 1H, CH$_2$C*H*$_2$NH), 7.14−7.31

(m, 10H, HNCH$_2$*Ph*), 11.25 (br, 1H, N*H*). $^{11}$B NMR (96.3 MHz, CD$_3$C$_6$D$_5$) $\delta$ −14.10 (2B), −23.41 (2B), −35.38 (2B), −38.36 (1B), −40.39 (1B), −45.71 (1B).

**24**: A procedure analogous to that used to prepare **23** was used, but starting from the complex **22** (0.28 g, 1.0 mmol). Yield: 0.24 g (75%). Mp: 148 °C (dec.). HRMS: Calcd for $[^{12}C_{13}{}^{11}B_9{}^1H_{27}{}^{14}N^{27}Al]^+$: 323.2796. Found: 323.2808. IR spectrum (KBr pellet, cm$^{-1}$) $\nu$(B−H) 2528, $\nu$(C−H) 2993, 3021, 3067. $^1$H NMR (300 MHz, CD$_3$C$_6$D$_5$) $\delta$ −0.37 (s, 3H, Al*Me*), 1.69 (s, 3H, C$_{cab}$*Me*), 1.99 (m, 1H, C*H*$_2$CH$_2$NH), 2.22 (m, 1H, C*H*$_2$CH$_2$NH), 3.42 (m, 1H, HNC*H*$_2$Ph), 3.55 (m, 1H, CH$_2$C*H*$_2$NH), 3.72 (m, 1H, HNC*H*$_2$Ph), 4.12 (m, 1H, CH$_2$C*H*$_2$NH), 7.21−7.39 (m, 10H, HNCH$_2$*Ph*), 10.38 (br, 1H, N*H*). $^{11}$B NMR (96.3 MHz, CD$_3$C$_6$D$_5$) $\delta$ −10.55 (3B), −21.53 (2B), −24.04 (3B), −46.85 (1B).

**Crystal Structure Determination.** Crystals of **3**, **5**, **6**, **7**, **14**, **18**, **19**, and **23** were obtained from toluene at −15 °C, sealed in glass capillaries under argon, and mounted on the diffractometer. Preliminary examination and data collection were performed using a Brucker SMART CCD detector system single-crystal X-ray diffractometer equipped with a sealed-tube X-ray source (40 kV × 50 mA) using graphite-monochromated Mo K$\alpha$ radiation ($\lambda$ = 0.7107 Å). Preliminary unit cell constants were determined with a set of 45 narrow-frame (0.3° in $\omega$) scans. The double-pass method of scanning was used to exclude any noise. The collected frames were integrated using an orientation matrix determined from the narrow-frame scans. The SMART software package was used for data collection, and SAINT was used for frame integration.[18a] Final cell constants were determined by a global refinement of xyz centroids of reflections harvested from the entire data set. Structure solution and refinement were carried out using the SHELXTL-PLUS software package.[18b]

**Computational Details.** Stationary points on the potential energy surface were calculated using the Amsterdam Density Functional (ADF) program, developed by Baerends et al.[19] and vectorized by Ravenek.[20] The numerical integration scheme applied for the calculations was developed by te Velde et al.[21] The geometry optimization procedure was based on the method due to Versluis and Ziegler.[22] The electronic configurations of the molecular systems were described by double-$\zeta$ STO basis sets with polarization functions for the H, N, C, and B atoms, while triple-$\zeta$ Slater type basis sets were employed for the Al atom.[23] The 1s electrons of N, C, and B, and the 1s−2p electrons of Al were treated as frozen cores. A set of auxiliary[24] s, p, d, f, and g STO functions, centered on all nuclei, was used in order to fit the molecular density and the Coulomb and exchange potentials in each SCF cycle. Energy differences were calculated by augmenting the local exchange-correlation potential by Vosko et al.[25] with Becke's[26] nonlocal exchange corrections and Perdew's[27] nonlocal correlation corrections (BP86). Geometries were optimized including nonlocal corrections at this level of theory. ZORA scalar relativistic corrections[28] were added variationally to the total energy for all

(19) (a) Baerends, E. J.; Ellis, D. E.; Ros, P. *Chem. Phys.* **1973**, *2*, 41. (b) Baerends, E. J.; Ros, P. *Chem. Phys.* **1973**, *2*, 52.

(20) Ravenek, W. In *Algorithms and Applications on Vector and Parallel Computers*; te Riele, H. J. J., Dekker, T. J., van de Horst, H. A., Eds.; Elsevier: Amsterdam, The Netherlands, 1987.

(21) (a) Boerrigter, P. M.; Velde, G. T.; Baerends, E. J. *Int. J. Quantum Chem.* **1988**, *33*, 87. (b) te Velde, G.; Baerends, E. J. *J. Comput. Chem.* **1992**, *99*, 84.

(22) Versluis, L.; Ziegler, T. *J. Chem. Phys.* **1988**, *88*, 322.

(23) (a) Snijders, J. G.; Baerends, E. J.; Vernoijs, P. *At. Nucl. Data Tables* **1982**, *26*, 483. (b) Vernoijs, P.; Snijders, J. G.; Baerends, E. J. *Slater Type Basis Functions for the Whole Periodic System*; Internal Report (in Dutch); Department of Theoretical Chemistry, Free University: Amsterdam, The Netherlands, 1981.

(24) Krijn, J.; Baerends, E. J. *Fit Functions in the HFS Method*; Internal Report (in Dutch); Department of Theoretical Chemistry, Free University: Amsterdam, The Netherlands, 1984.

(25) Vosko, S. H.; Wilk, L.; Nusair, M. *Can. J. Phys.* **1980**, *58*, 1200.

(26) (a) Becke, A. *Phys. Rev. A* **1988**, *38*, 3098. (b) Becke, A. D. *J. Chem. Phys.* **1993**, *98*, 1372. (c) Becke, A. D. *J. Chem. Phys.* **1993**, *98*, 5648.

systems. In view of the fact that all systems investigated in this work show a large HOMO−LUMO gap, a spin-restricted formalism was used for all calculations. No symmetry constraints were used.

**Supporting Information Available:** Crystallographic data for the structures **3**, **5**, **6**, **7**, **14**, **18**, **19**, and **23** and listings giving optimized geometries of the crucial structures (**C**, **D**, **5**, and **5′**) reported (Cartesian coordinates, in Å). This material is available free of charge via the Internet at http://pubs.acs.org.

JA802163Q

(27) (a) Perdew, J. P. *Phys. Rev. B* **1986**, *34*, 7406. (b) Perdew, J. P. *Phys. Rev. B* **1986**, *33*, 8822.

(28) (a) van Lenthe, E.; Baerends, E. J.; Snijders, J. G. *J. Chem. Phys.* **1993**, *99*, 4597. (b) van Lenthe, E.; Ehlers, A. E.; Baerends, E. J. *J. Chem. Phys.* **1999**, *110*, 8943.